Progress in Retinal and Eye Research 97 (2023) 101207

Contents lists available at ScienceDirect

Progress in Retinal and Eye Research

journal homepage: www.elsevier.com/locate/preteyeres

Latest advances in white spot syndromes: New findings and interpretations

Maria Vittoria Cicinelli [a,b,*], Prithvi Ramtohul [c,d], Alessandro Marchese [a,b,e], Francesco Bandello [a,b], K. Bailey Freund [c,d], Elisabetta Miserocchi [a,b], Lee M. Jampol [e]

[a] School of Medicine, Vita-Salute San Raffaele University, Milan, Italy
[b] Department of Ophthalmology, IRCCS San Raffaele Scientific Institute, Milan, Italy
[c] Vitreous Retina Macula Consultants of New York, New York, NY, USA
[d] NYU Grossman School of Medicine, New York, NY, USA
[e] Department of Ophthalmology, Feinberg School of Medicine, Northwestern University, Chicago, IL, USA

ARTICLE INFO

Keywords:
White spot syndromes
Acute zonal occult outer retinopathy
Multiple evanescent white dot syndrome
Multifocal choroiditis
Choroidal neovascularization
Punctate inner choroidopathy

ABSTRACT

White spot syndromes (WSS) pose challenges in the field of ophthalmology, particularly in terms of accurate diagnosis and effective management. However, recent advancements in multimodal imaging (MMI) have significantly contributed to our understanding of WSS, allowing for improved characterization of these inflammatory chorioretinopathies. By employing various imaging modalities, including fundus fluorescein angiography, indocyanine green angiography, fundus autofluorescence, optical coherence tomography (OCT), ultra-widefield imaging, and OCT angiography, researchers and clinicians have gained valuable insights into the underlying pathophysiological changes and clinical progression of WSS.

Furthermore, MMI has unveiled novel and atypical variants within the spectrum of WSS, expanding our knowledge in this field. Notably, the identification of secondary forms of WSS occurring concurrently with unrelated chorioretinal disorders has suggested a potential autoimmune mechanism underlying these conditions. The introduction of MMI has also facilitated a more comprehensive evaluation of previously ill-defined entities, such as acute zonal occult outer retinopathy, leading to improved diagnostic criteria and enhanced recognition of distinct features. This review paper provides a comprehensive overview of the latest advances and interpretations in WSS. By integrating MMI into the diagnosis and management of these conditions, this review aims to enhance patient outcomes and provide valuable insights into the complexities surrounding WSS.

1. Introduction

White spot syndromes (WSS) present significant challenges in terms of diagnosis, management, and patient care. The advent of multimodal imaging (MMI) has played a crucial role in uncovering new aspects of WSS and providing a comprehensive understanding of these inflammatory chorioretinopathies.

Utilizing various imaging techniques such as fluorescein angiography (FA), indocyanine green angiography (ICGA), fundus autofluorescence (FAF), optical coherence tomography (OCT), ultra-widefield (UWF) imaging, and OCT angiography (OCTA), researchers and clinicians have gained valuable insights into WSS. While the exact underlying immune mechanism remains uncertain, this multidimensional approach has allowed for a detailed evaluation of clinical changes, disease progression, and the identification of novel or atypical variants.

WSS primarily affect otherwise healthy individuals, with a higher prevalence among young and middle-aged females. However, recent research has highlighted the interplay between WSS, such as multiple evanescent white dot syndrome (MEWDS) and punctate inner choroidopathy/idiopathic multifocal choroiditis (PIC/iMFC), and other chorioretinal disorders. It has become evident that these conditions can coexist or occur sequentially, even if they appear unrelated. Furthermore, the emergence of secondary WSS cases has strengthened the hypothesis that these syndromes are autoimmune disorders, possibly triggered by antigens originating from the outer retina or inner choroid.

The introduction of the concept of acute zonal occult outer retinopathy (AZOOR)-related complex diseases by Gass (Gass, 1993) in ophthalmic literature has sparked debates regarding the definition of the original entity. As a result, AZOOR has become a broad diagnostic term encompassing a range of chorioretinal diseases with varying patterns of photoreceptor damage, leading to inconsistent understanding. The utilization of MMI has facilitated a more comprehensive assessment of this

* Corresponding author. Department of Ophthalmology, IRCCS San Raffaele Scientific Institute, Via Olgettina 60, Milan, 20132, Italy.
E-mail address: Cicinelli.mariavittoria@hsr.it (M.V. Cicinelli).

https://doi.org/10.1016/j.preteyeres.2023.101207
Received 22 June 2023; Received in revised form 8 August 2023; Accepted 8 August 2023
Available online 12 August 2023
1350-9462/© 2023 Elsevier Ltd. All rights reserved.

List of abbreviations

AIBSE	acute idiopathic blind spot enlargement
AZOOR	acute zonal occult outer retinopathy
BrM	Bruch's membrane
CNV	choroidal neovascularization
ELM	external limiting membrane
ERG	electroretinogram
ERP	early receptor potential
EZ/IZ	ellipsoid zone/interdigitation zone
FA	fluorescein angiography
FAF	fundus autofluorescence
ICGA	indocyanine green angiography
IL	interleukin
MEWDS	multiple evanescent white dot syndrome
mfERG	multifocal electroretinogram
MMI	multimodal imaging
MORR	multi-zonal outer retinopathy and retinal pigment epitheliopathy
OCT	optical coherence tomography
OCTA	OCT angiography
ONL	outer nuclear layer
OPL	outer plexiform layer
PIC/iMFC	punctate inner choroidopathy/idiopathic multifocal choroiditis
POHS	presumed ocular histoplasmosis syndrome
PXE	pseudoxanthoma elasticum
RPE	retinal pigment epithelium
SUN	Standardization of Uveitis Nomenclature
TNF	tumor necrosis factor
UWF	ultra-widefield
VEGF	vascular endothelial growth factor
WSS	white spot syndromes

disease, establishing more precise diagnostic criteria and enhancing the recognition of its distinctive features.

This review aims to provide a comprehensive evaluation of the latest findings and interpretations of WSS, namely MEWDS, PIC/iMFC, and AZOOR, bringing us closer to understanding the complexities of these diseases and improving patient outcomes. We will not discuss placoid diseases, as our group has recently conducted a detailed review on this topic, covering serpiginous choroiditis, acute posterior multifocal placoid pigment epitheliopathy, and relentless placoid chorioretinitis (Marchese et al., 2022a). Moreover, acute macular neuroretinopathy has been excluded from the review, as it is now recognized as a vascular disorder rather than an inflammatory condition (Cabral et al., 2022).

2. PIC/iMFC

2.1. Background

2.1.1. Historical background

In 1969, Krill et al. described a new condition called "*multifocal inner choroiditis*" characterized by multiple chorioretinal lesions and choroidal neovascularization (CNV) in patients with a positive histoplasmin skin test (Krill et al., 1969). The condition was later called presumed ocular histoplasmosis syndrome (POHS), which exhibits distinct characteristics from other choroidal disorders (Smith and Ganley, 1972). POHS specifically refers to multifocal chorioretinal scarring in areas of the United States where Histoplasma is endemic (Woods and Wahlen, 1959). POHS does not show anterior segment inflammation or vitritis, is not associated with a specific sex or myopic predilection, presents later in life, and has a high risk of developing CNV and presumably granulomatous hilar adenopathy and/or calcifications on chest x-ray films (Parnell et al., 2001).

In 1973, Nozik and Dorsch identified a similar chorioretinopathy associated with anterior chamber inflammation and vitritis in two patients with no evidence of infectious disease (Nozik and Dorsch, 1973). In 1984, Dreyer and Gass described a series of 28 patients with anterior and vitreous inflammation and multifocal deep yellowish lesions (>250 μm), presumed to be inflammatory and evolving into punched-out pigmented chorioretinal scars (Dreyer and Gass, 1984). This condition was named "multifocal choroiditis with panuveitis", which today is considered a form of iMFC. The same year, Watzke et al. outlined a clinical syndrome affecting 10 young, otherwise healthy, myopic women characterized by small (100–300 μm), yellow-grey lesions at the posterior pole that progressed to atrophic chorioretinal scars (Watzke et al., 1984). Most patients had bilateral involvement and developed CNV, and no evidence of histoplasmosis infection was found. This syndrome was labeled as "punctate inner choroidopathy."

2.1.2. Terminology: the alphabet soup of PIC, iMFC, pseudo-POHS, and others

Multifocal choroiditis is a broad term encompassing various disorders characterized by multiple choroidal or chorioretinal lesions caused by infectious, inflammatory, or infiltrative conditions. These conditions may include tuberculosis, histoplasmosis, syphilis, brucellosis, coccidiomycosis, candidiasis, sarcoidosis, vitreoretinal lymphoma, and other granulomatous diseases (Essex et al., 2013; Marchese et al., 2022b). When these underlying conditions are ruled out, a diagnosis of iMFC is considered. Traditionally, the term PIC has been used to describe mild localized cases restricted to the macular region without vitritis (Essex et al., 2013; Gilbert et al., 2020; Spaide et al., 2013). There is ongoing debate regarding the distinction between iMFC and PIC, but we consider PIC synonymous with iMFC.

Several alternative names have been used in the literature to describe various presentations of iMFC. These include pseudo-POHS (Callanan and Gass, 1992), recurrent multifocal choroiditis (Morgan and Schatz, 1986), multifocal choroidopathy (Ongkosuwito et al., 1999), disseminated inner choroiditis (Saraux et al., 1986), and hemorrhagic macular choroidopathy (Flage et al., 1977). The term pseudo-POHS was coined by Callanan and Gass to describe a clinical entity resembling POHS in individuals from areas where Histoplasma is not endemic (Callanan and Gass, 1992). However, it is now recommended to use the term iMFC instead (Essex et al., 2013). Additionally, the eponym "progressive subretinal fibrosis" has been introduced to describe a very rare inflammatory choroiditis characterized by the presence of whitish fibrotic subretinal lesions that progressively enlarge and merge together (Cantrill and Folk, 1986; Palestine et al., 1984). Thus, it may refer to severe cases of iMFC.

2.1.3. Clinical features and classification criteria

The Standardization of Uveitis Nomenclature (SUN) working group recently utilized machine learning to establish diagnostic criteria for PIC (Standardization of Uveitis Nomenclature Working, 2021b) and iMFC (Standardization of Uveitis Nomenclature Working, 2021a). The key criteria for diagnosing PIC include the presence of small (<250 μm), punctate, multifocal choroidal inflammatory lesions in the posterior pole, with or without involvement of the mid-periphery. Additionally, minimal or absent anterior chamber and vitreous inflammation are observed (Standardization of Uveitis Nomenclature Working, 2021b) (Fig. 1).

On the other hand, the key criteria for diagnosing iMFC include the presence of large (>125 μm), oval or round-shaped, multifocal choroidal

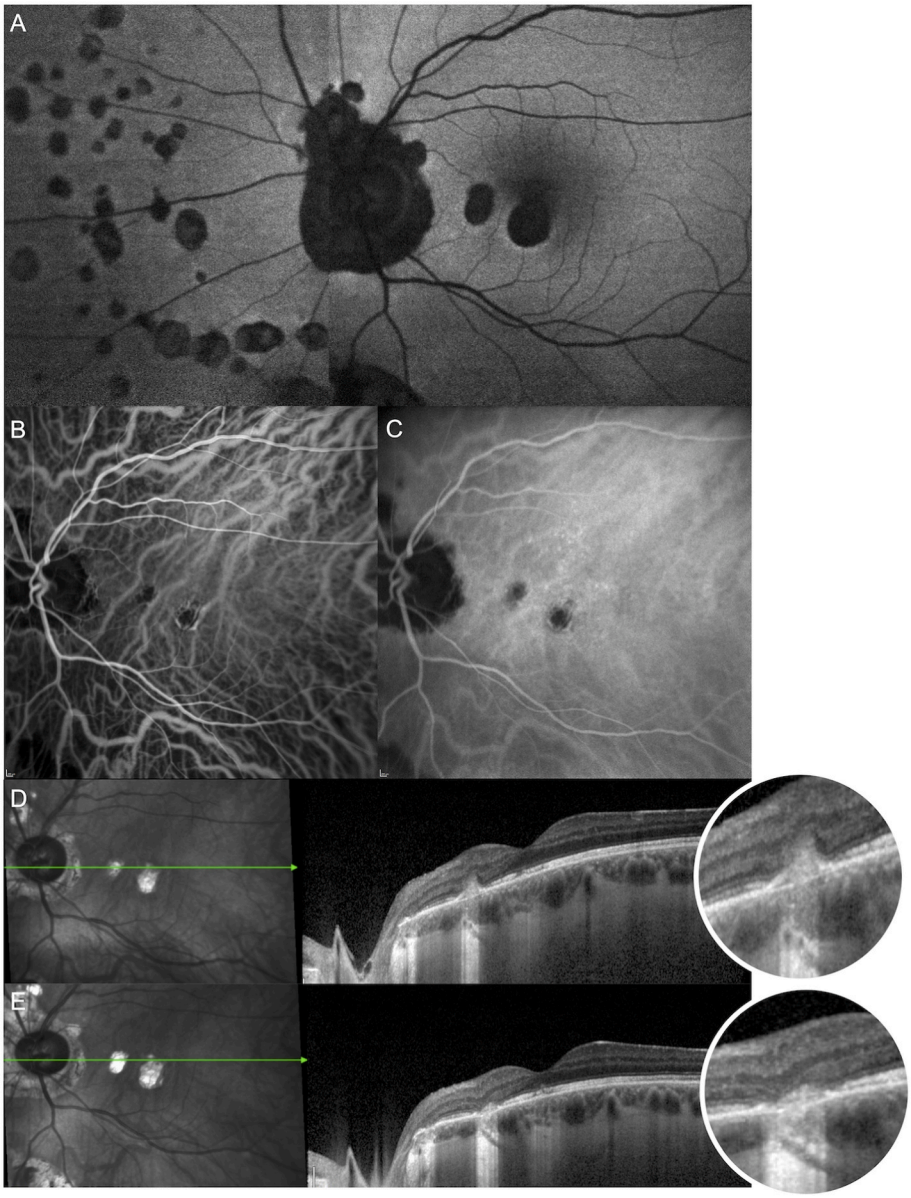

Fig. 1. Representative case of punctate inner choroidopathy/idiopathic multifocal choroiditis (PIC/iMFC) in a highly myopic patient. A. Fundus autofluorescence (FAF) image of the left eye of a myopic male in his 40s (refractive error: −9.00 diopters) reveals peripapillary retinal pigment epithelium (RPE) atrophy and multiple punched-out spots of hypo-autofluorescence in the mid-periphery and macular area, corresponding to RPE and outer retinal atrophy. Faint hyperautofluorescence surrounds the spots. B. Early-phase indocyanine green angiography (ICGA) demonstrates normal choroidal filling and two hypofluorescent spots in the macula, indicating the presence of inflammatory material. Increased visibility of deeper choroidal vessels around the lesions is observed. C. Late-phase ICGA shows persistent hypofluorescent spots in the macula, along with faint hyperfluorescence in the macular area, possibly indicating choroidal hyperpermeability. D. Optical coherence tomography (OCT) B-scan through the macula (green line) illustrates an active choroiditis spot. The PIC/iMFC lesion is characterized by subretinal isoreflective material that splits the RPE/Bruch's membrane (BrM) complex (see magnification), resulting in posterior deflection of the BrM and choroidal hypertransmission. Focal choroidal thickening beneath the lesion with loss of the normal vascular texture is observed. Co-registered near-infrared (NIR) imaging reveals two hyperreflective spots corresponding to patchy chorioretinal atrophy. E. Tracked OCT B-scan through the fovea acquired after one month depicts the choroiditis spot during the resolution phase. Partial disappearance of the subretinal isoreflective material and enlargement of the posterior signal hypertransmission are observed (see magnification). The choroid appears thinner. Co-registered NIR imaging shows enlargement of the two hyperreflective spots.

inflammatory lesions with punched-out atrophic chorioretinal scars. These lesions are found in the mid-periphery or far-periphery, with or without the involvement of the posterior pole, and exhibit evidence of vitreous inflammation (Standardization of Uveitis Nomenclature Working, 2021a).

In cases of PIC/iMFC, linear streaks or Schlaegel lines can also be observed, primarily in the mid-periphery near the equator (Fig. 2). These streaks are commonly seen in young women with high and rapidly progressive myopia, often in conjunction with other PIC/iMFC lesions (Chen et al., 2022). The mechanisms of formation of Schlaegel lines is unknown but may be triggered by a combination of inflammatory insults and axial elongation of the eyeball, resulting in tangential pressure on the retinal pigment epithelium (RPE).

PIC/iMFC may also present with peripapillary chorioretinal scarring and atrophy resembling serpiginous choroiditis (Moussa et al., 2022) (Fig. 3). It is important to differentiate this peripapillary chorioretinal atrophy from other degenerative diseases, such as lacquer cracks or angioid streaks. Identification of classic ophthalmoscopic findings of PIC/iMFC, including multiple yellowish inflammatory lesions, punched-out chorioretinal scars, or Schlaegel lines, can assist in making the diagnosis. Exclusion criteria involve positive infectious tests or evidence of granulomatous diseases, such as tuberculosis and sarcoidosis.

Secondary CNV occurs in up to 83% of PIC/iMFC lesions (Zahid et al., 2017) and is reported as the most common cause of vision loss in these patients. The reported incidences of visual impairment (20/50 or worse) and blindness (20/200 or worse) are 0.19/eye-year and 0.12/eye-year, respectively (Thorne et al., 2006).

2.1.4. *Pathogenesis*

PIC/iMFC is believed to be autoimmune, and the presence of the condition in siblings or successive generations suggests a potential familial association in its development (Levine et al., 2008; Sugawara et al., 2010). Furthermore, the high prevalence of autoimmune diseases in personal (13%) or family histories (21%) further supports the hypothesis of a genetic predisposition to PIC/iMFC (Atan et al., 2011; Gerstenblith et al., 2007). Individuals with WSS may have systemic immune dysregulation, although the specific genes or haplotypes responsible for genetic susceptibility have not been definitively identified (Pearlman et al., 2009).

Patients with PIC/iMFC exhibit a distinct human leukocyte antigen

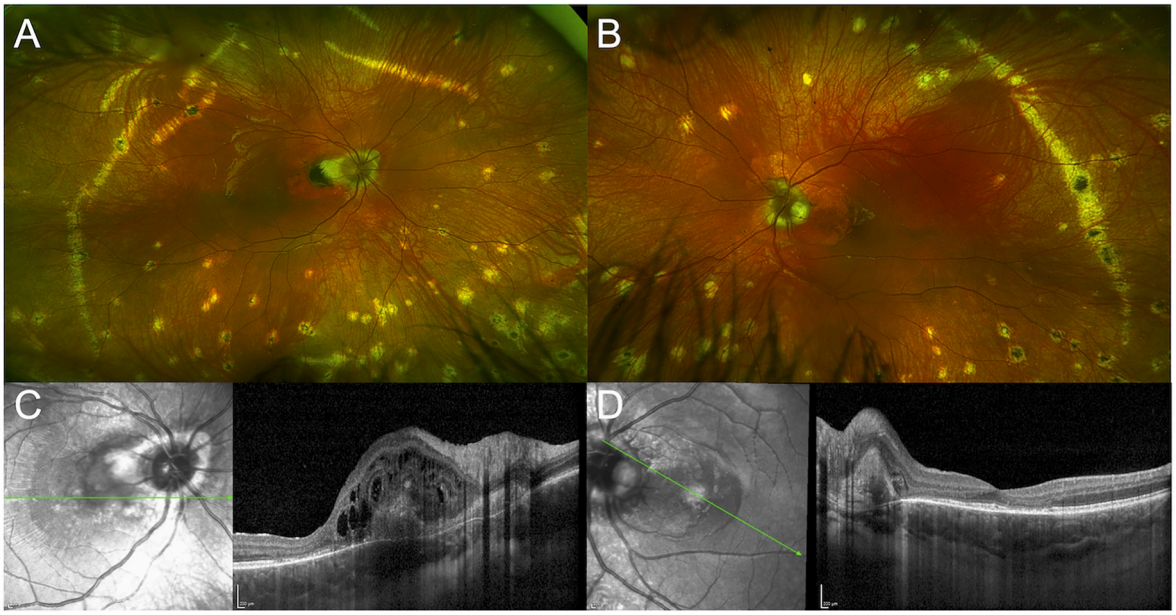

Fig. 2. Idiopathic multifocal choroiditis with bilateral Schlaegel lines and choroidal neovascularization (CNV). A. Color fundus photograph of the right eye (OD) shows chorioretinal lesions and linear streaks of punched-out chorioretinal atrophy in the mid and far-periphery. Peripapillary atrophy with a pigmented solid lesion is observed. In the macula, a large area of retinal pigment epithelium (RPE) atrophy is present, with increased visualization of choroidal vessels approaching the fovea. B. Color fundus photograph of the left eye (OS) reveals similar chorioretinal lesions and linear streaks of punched-out chorioretinal atrophy in the mid and far-periphery. Peripapillary atrophy is also observed. In the macula, there is a large area of RPE atrophy involving the fovea. C. Optical coherence tomography (OCT) through the fovea of the OD demonstrates increased retinal thickness due to a subretinal hyperreflective lesion with fuzzy margins, corresponding to the CNV. Intraretinal fluid and disruption of the perilesional ellipsoid zone (EZ) layer are observed. The choroid appears thick. D. OCT through the fovea of the OS shows a subretinal hyperreflective lesion with well-defined margins in the peripapillary area. Disruption of the EZ is observed around the lesion and under the fovea.

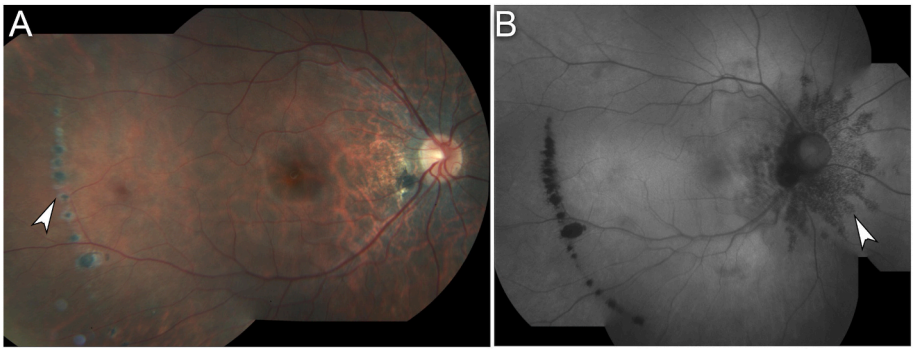

Fig. 3. Idiopathic multifocal choroiditis with peripapillary chorioretinal atrophy resembling serpiginous-like choroiditis. A. Color fundus photograph of the right eye shows peripapillary hypopigmentation and atrophy, allowing visualization of the choroidal vessels. In the peripheral region, multiple punched-out lesions of chorioretinal atrophy and hyperpigmentation are observed, forming a Schlaegel line (white arrow). B. Fundus autofluorescence image reveals peripapillary hypo-autofluorescence characterized by a radial pattern (white arrow), along with hypo-autofluorescence corresponding to the peripheral punched-out chorioretinal lesions.

(HLA) profile compared to those with POHS. Haplotype analysis of PIC/iMFC patients has revealed a unique pattern with decreased frequencies of *HLA-DR2* and *HLA-B7*, while patients with POHS show an increased prevalence of these antigens (Meredith et al., 1978; Spaide et al., 1990).

Targeted genotyping of PIC/iMFC patients has demonstrated an association with specific tumor necrosis factor (TNF) loci and interleukin (IL)-10 haplotypes when compared to a healthy control population (Atan et al., 2011). Interestingly, the same haplotype-tagged single nucleotide polymorphisms have previously been linked to non-infectious uveitis (Atan et al., 2010). However, the study found no significant differences between iMFC and PIC patients at any IL10 or TNF locus investigated, suggesting that genotype alone cannot distinguish between the two conditions, which may represent two manifestations of the same disease.

Finally, there is a strong association between complement factor H polymorphisms and PIC/iMFC, suggesting abnormal regulation of the alternative complement pathway (Ferrara et al., 2008).

2.1.5. Pathology

Most histopathological investigations are limited because tissue samples are generally restricted to excised subfoveal CNV membranes (Olsen et al., 1996; Pachydaki et al., 2012; Shimada et al., 2008). In a clinicopathologic correlation study of a young deceased patient diagnosed with PIC/iMFC, Dunlop et al. described perivascular chronic inflammatory infiltrates in the choroid consisting mainly of B and T lymphocytes (Dunlop et al., 1998).

2.2. Imaging findings of PIC/iMFC

2.2.1. OCT features

Vance et al. were the first to report the spectral-domain OCT (SD-OCT) characteristics of active PIC/iMFC lesions, which corresponded to the presence of homogeneous sub-RPE material of medium reflectivity associated with choroidal hyperreflectivity and vitreous cells (Vance et al., 2011b). The posterior choroidal hyperreflectivity was attributed to the disruption of photoreceptors and RPE by the inflammatory infiltrates.

A 5-stage classification system of PIC/iMFC lesions was then proposed using SD-OCT, showing a sequential progression from choroidal infiltration to sub-RPE nodule, chorioretinal nodule, regression, and retinal herniation (Zhang et al., 2013). Using enhanced depth imaging OCT, focal variations in choroidal thickness have been reported, with acute lesions showing choroidal thickening and resolved lesions showing choroidal thinning (Spaide et al., 2013; Zarranz-Ventura et al., 2014). Some patients may present with focal choroidal excavation (FCE), which is a choroidal concavity without posterior staphyloma or scleral ectasia, plausibly due to atrophic scarring of the inner choroid (Kim et al., 2015).

Newly recognized OCT features include focal hyporeflectivity and loss of the normal choroidal architecture below the active lesion, splitting of the RPE/Bruch's membrane (BrM), and a posterior deflection of the BrM (Abdelhakim et al., 2021) (Fig. 1). These findings may support the hypothesis that the inflammatory process primarily affects the RPE/BrM complex. However, the exact site of inflammation remains unknown, and it is uncertain whether inflammation originates from the RPE/BrM complex or the choriocapillaris. The contribution of the choroid to the pathogenesis of PIC/iMFC is also uncertain.

RPE disruption and choroidal hypertransmission may suggest secondary CNV (Chen et al., 2021; Shi et al., 2020). Inflammatory CNV can be accompanied by multiple finger-like projections extending from the active CNV into the outer retina, referred to as the "pitchfork sign," as well as focal choroidal thickening underlying the CNV (Giuffre et al., 2021; Hoang et al., 2013a). Inflammatory CNV may develop at the same site as FCE, and the CNV may precede or follow the formation of FCE (Haas et al., 2020). Intraretinal cavitations can be detected in the restoration stage and should be differentiated from exudation from the CNV (Atan et al., 2011; Gan et al., 2020).

2.2.2. OCTA features

In patients with active inflammatory lesions, OCTA can provide valuable insights by revealing choroidal flow voids that tend to normalize when the inflammation subsides. These flow voids are often accompanied by RPE disruption and subretinal hyperreflective material, as observed on structural OCT scans (Zahid et al., 2017).

In addition to assessing inflammatory lesions, OCTA helps detect CNV, as active PIC/iMFC lesions and secondary CNV can present similar findings on OCT and FA (Baumal et al., 2015; Dutheil et al., 2018). OCTA demonstrates a lacy network of vessels in the outer retina on en-face slabs and blood flow signal on corresponding B-scans. Neovascular flow often persists during disease quiescence, so its presence may not prove disease activity. However, OCTA may show shrinkage of the CNV network following injections of anti-vascular endothelial growth factor (VEGF) agents (de Groot et al., 2023; Kongwattananon et al., 2022). OCTA may also enable the detection of centripetal restoration of the choriocapillaris flow signal after immunosuppressive therapy (Nakao et al., 2016; Thompson et al., 2021).

2.2.3. FAF features

On FAF imaging, active and inactive PIC/iMFC lesions exhibit hypo-FAF due to RPE disruption (Haen and Spaide, 2008). Several patterns of hyper-FAF occurring concurrently with active PIC/iMFC lesions have been reported. These patterns range from discrete hyper-FAF halos surrounding active lesions to patchy hyper-FAF lesions, peripapillary hyper-FAF rings, or more diffuse zonal hyper-FAF (Gattoussi et al., 2018; Jung et al., 2014; Kaden et al., 2019; Kramer and Priel, 2014; Li et al., 2015; Munk et al., 2015). These hyper-FAF lesions may relate to the unmasking of RPE FAF signal due to reduced photopigment in damaged, absent, or dysfunctional photoreceptors (Freund et al., 2013). hyper-FAF may also result from RPE hyperplasia or hyper-FAF materials in the subretinal space. hyper-FAF can be associated with relative scotomata and enlarged blind spot (Jung et al., 2014; Kaden et al., 2019; Munk et al., 2015; Riaz et al., 2012). The detection of perilesional hyper-FAF can be employed to monitor PIC/iMFC recurrences (Gan et al., 2020) and may predict the treatment response to corticosteroids (Turkcuoglu et al., 2011).

2.2.4. FA and ICGA features

On FA, active PIC/iMFC lesions typically appear hypofluorescent in early frames due to the displacement of choroidal fluorescence but exhibit late leakage and staining in the late frames (Dreyer and Gass, 1984; Morgan and Schatz, 1986). Inactive PIC/iMFC lesions are hyperfluorescent in all phases due to RPE window defects (Altan-Yaycioglu et al., 2006). Secondary CNV can be detected on FA as a well-demarcated area of hyperfluorescence in early frames followed by late leakage (Altan-Yaycioglu et al., 2006). However, it can be diagnostically challenging to differentiate CNV from inflammatory lesions. In these cases, OCTA has shown higher sensitivity than FA in identifying the neovascular network (de Groot et al., 2023; Kongwattananon et al., 2022).

On ICGA, both active and inactive PIC/iMFC lesions appear hypofluorescent in all phases (Altan-Yaycioglu et al., 2006). Associated findings include the visibility of deeper choroidal vessels under the choroidal lesions and the dilation and leakage of adjacent choroidal vessels. In some cases, late-phase ICGA reveals large spots of hypofluorescence not visible clinically or on FA and corresponding to secondary MEWDS (Slakter et al., 1997; Vadala et al., 2001) (see paragraph 4.C).

2.3. Novel PIC/iMFC phenotypes and associations

2.3.1. Chrysanthemum

A rare subtype of PIC/iMFC was recently described by Ramtohul et al., characterized by a distinctive lesion morphology resembling a chrysanthemum (Ramtohul et al., 2023b). On ophthalmoscopic examination, chrysanthemum lesions exhibit a grey-yellow central lesion known as the core, surrounded by pale satellite dots resembling petals (Fig. 4). OCT imaging of the chrysanthemum phenotype reveals subretinal iso/hyperreflective material splitting the RPE/BrM complex, defects in the RPE/BrM complex, a downwardly deflected BrM, and posterior choroidal hypertransmission within the core. Noteworthy characteristics of the chrysanthemum phenotype include a high number of lesions (more than 20 lesions in 56% of eyes), involvement of the mid- and far-peripheral regions (52% of eyes), and a frequent occurrence of secondary MEWDS (60% of eyes) (see paragraph 4.C).

2.3.2. PIC/iMFC in highly myopic eyes

Hady et al. demonstrated that 11% of patients with pathological myopia exhibited OCT features of active PIC/iMFC lesions during a follow-up period of 68.3 ± 40.3 months (range 12–156 months) (Hady et al., 2022). PIC/iMFC lesions in highly myopic eyes can increase the risk of CNV and patchy chorioretinal atrophy. Managing PIC/iMFC lesions in highly myopic eyes may require corticosteroids and anti-VEGF agents to control CNV and inflammation. In recurrent episodes, longer-term immunosuppressive therapies may be necessary to prevent complications and the development of chorioretinal atrophy (Airaldi et al., 2023).

2.3.3. Zonal outer retinal atrophy and chorioretinal atrophy

Jung et al. described a series of eyes presenting with zonal areas of outer retina, RPE, and choroidal atrophy associated with PIC/iMFC lesions (Jung et al., 2014) (Fig. 5). These changes were persistent, and the author hypothesized that chorioretinal atrophy resulted from recurrent episodes of acute inflammation. The use of corticosteroids and other immunosuppressive therapies may help limit relapses and slow the progression, but the effectiveness of such treatments is uncertain.

Munk et al. reported a variant of PIC/iMFC and chorioretinal atrophy, which led to decreased visual acuity and scotomata with severe vision loss up to hand motion. The decrease in visual acuity and visual field loss was attributed to central photoreceptor attenuation,

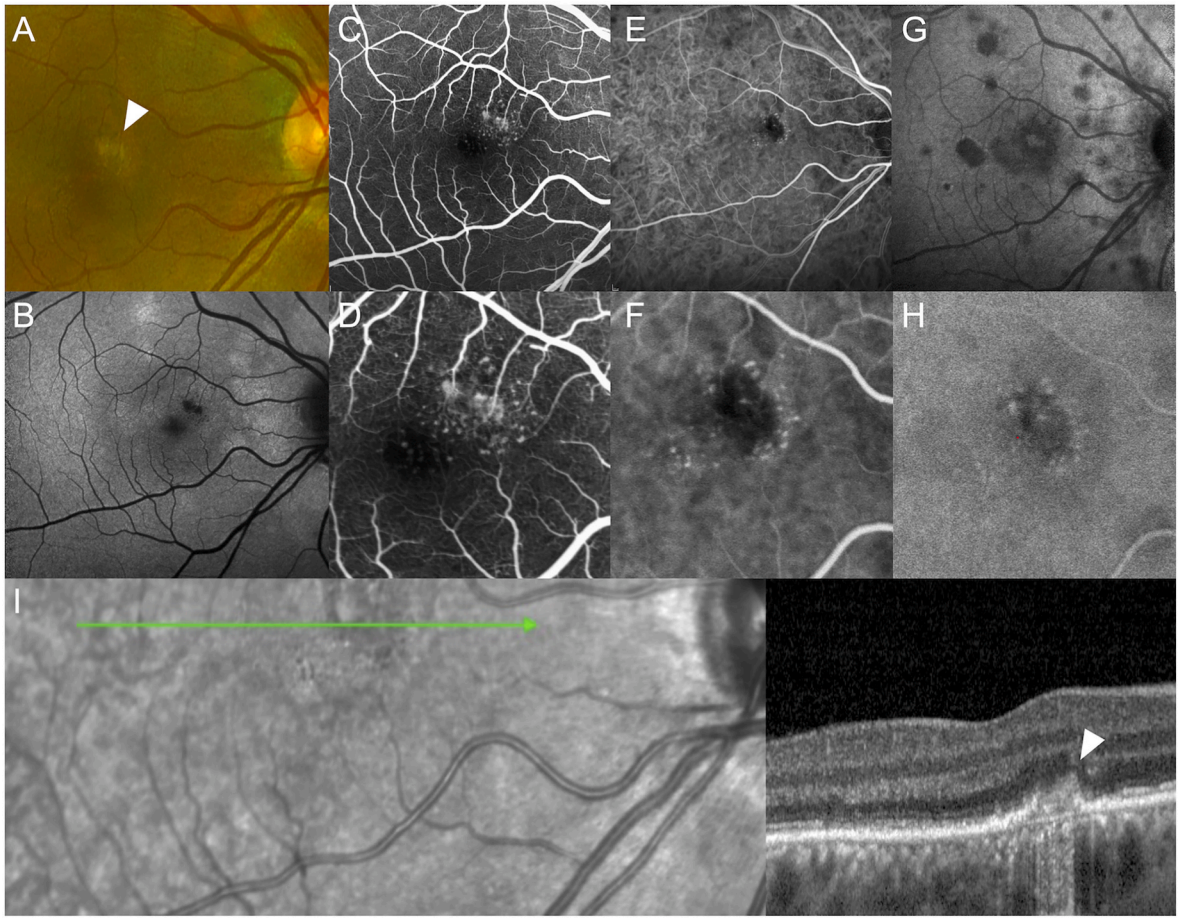

Fig. 4. Multimodal imaging of a macular chrysanthemum lesion. A. Baseline color fundus photography reveals a macular chrysanthemum lesion characterized by a grey-yellow central lesion (the core) surrounded by pale satellite dots resembling petals (white arrowhead). B. Fundus autofluorescence image displays a hypo-autofluorescent chrysanthemum lesion in the macula surrounded by faint hyperautofluorescence in the peripapillary area and superior to the macula. C-D (magnification). Fluorescein angiography shows a central hyperfluorescent lesion surrounded by dotted hyperfluorescence. E-F (magnification). Early-frame indocyanine green angiography (ICGA) of the lesion shows early hypofluorescence of the central lesion (core) surrounded by dotted hyperfluorescence. G-H (magnification). Late-frame ICGA reveals faded hyperfluorescence of the lesion. Notably, new spots of hypofluorescence become visible in the macula and peripapillary area, suggestive of secondary multiple evanescent white spot syndrome. I. OCT B-scan demonstrates subretinal hyperreflective material splitting the retinal pigment epithelium/Bruch's membrane complex, along with posterior choroidal hypertransmission (white arrowhead).

manifesting as areas of hyper-FAF and alterations of the EZ/IZ on OCT (Munk et al., 2015). The recovery of photoreceptors varied, ranging from total restoration of the outer retina and improvement in visual acuity to persistent damage and visual impairment.

We propose that outer retinal disruption in active PIC/iMFC may exhibit different patterns of evolution (Kaden et al., 2019). Reversible functional and outer retinal changes should be classified as secondary MEWDS, while persistent cases can be regarded as zonal retinochoroidal atrophy. Assessing the integrity of the outer retinal layers using OCT and FAF imaging and monitoring changes over time may have therapeutic and prognostic implications for patients with PIC/iMFC.

2.3.4. PIC/iMFC in pachychoroid disease eyes

The pachychoroid disease spectrum encompasses various disorders characterized by choroidal vascular alterations observed on multimodal imaging. These alterations include dilated choroidal veins (pachyveins), collaterals between vortex vein systems, inner choroidal thinning, increased choroidal thickness on OCT, and choroidal vascular hyperpermeability on late-phase ICGA (Cheung et al., 2019). Ultra-widefield ICGA and en-face OCT of the vortex vein system have suggested that choroidal venous outflow abnormalities may be a common mechanism of pachychoroid disorders, leading to congestion and inadequate blood flow (Bacci et al., 2022; Pang et al., 2014; Ramtohul et al., 2023a).

Through unsupervised machine learning and cluster analysis, our research team identified a distinct cluster of PIC/iMFC patients characterized by a young age, emmetropic or low myopia, thick choroids, choroidal vascular hyperpermeability on ICGA, chrysanthemum lesions, and a high frequency of FCE and subretinal fibrosis. These clinical and MMI characteristics overlap with those observed in the pachychoroid disease spectrum (Cheung et al., 2019) (Figs. 6–7). Therefore, we coined the term "punctate inner pachychoroidopathy" for this subtype (Ramtohul et al., under review).

We hypothesize that abnormal choroidal venous outflow may predispose to or enhance local inflammation, either through a pro-inflammatory environment or by impairing the clearance of inflammatory cells and cytokines (Smith, 1999). Treating patients with punctate inner pachychoroidopathy with corticosteroids during active disease is beneficial due to the rapid resolution of inflammatory lesions (Ramtohul et al., under review). However, a reduction in choroidal thickness, often considered an indicator of resolved choroidal inflammation, may not reliably indicate treatment response in these patients (Spaide et al., 2013).

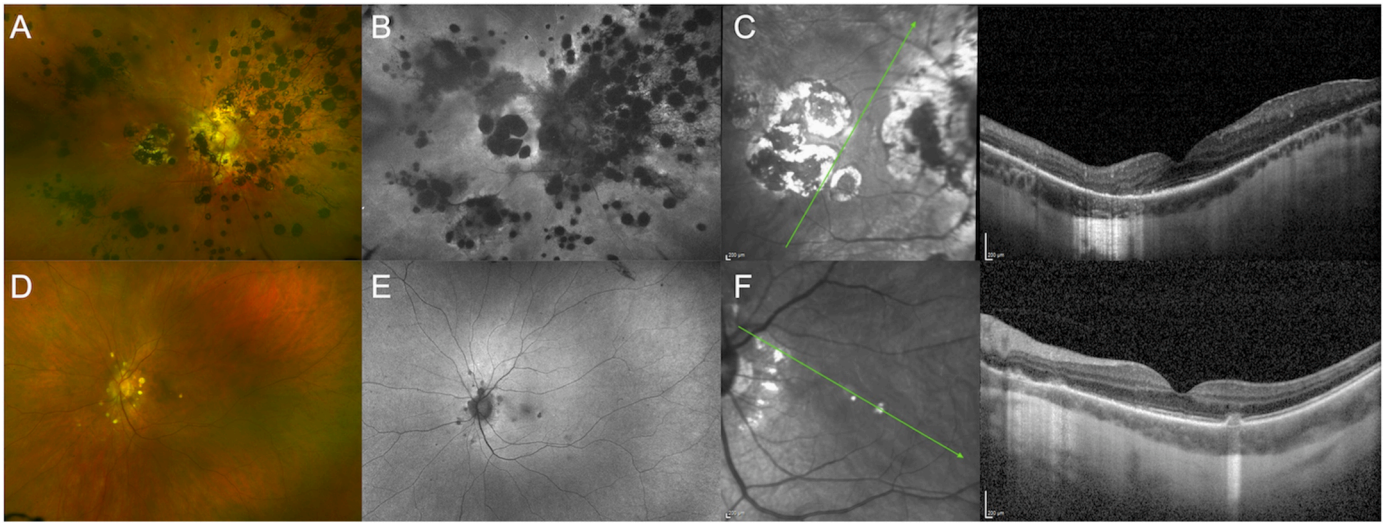

Fig. 5. Idiopathic multifocal choroiditis with bilateral multizonal outer retinal and chorioretinal atrophy.
A. Color fundus photography of the right eye (OD) demonstrates punched-out chorioretinal lesions in the mid- and far-periphery, accompanied by migration of pigment into these zones. Additionally, there is pronounced macular and peripapillary atrophy with pigment accumulation. B. Fundus autofluorescence imaging of OD displays multiple geographic zones of hypoautofluorescence within the areas of atrophy, along with ill-defined hyperautofluorescence surrounding the zones of macular and peripapillary atrophy. C. Optical coherence tomography (OCT) through the fovea of OD demonstrates perifoveal loss of the ellipsoid layer, outer photoreceptors, and disruption of the retinal pigment epithelium (RPE) with choroidal hypertransmission. Notably, the subfoveal area appears unaffected. D. Color fundus photography of the left eye (OS) reveals a few punched-out chorioretinal lesions in the peripapillary area. E. Fundus autofluorescence imaging of OS shows multiple small zones of atrophy sparing the central macula. F. OCT through the fovea of OS reveals multiple lesions characterized by subretinal hyperreflective material splitting the RPE/Bruch's membrane complex, accompanied by posterior choroidal hypertransmission.

3. MEWDS

3.1. Background

3.1.1. Historical background

Multiple evanescent white dot syndrome, first described by Jampol et al., in 1983, is an inflammatory disease primarily affecting the outer retina. It predominantly affects young-to-middle-aged females and may be preceded by flu-like symptoms (Baglivo et al., 1996; Gargouri et al., 2022). Some patients may have a personal or family history positive for systemic autoimmune disease (Pearlman et al., 2009; Ramakrishnan et al., 2021). There appears to be no racial predilection (Ramakrishnan et al., 2021). Classic symptoms of MEWDS include blurred vision, photopsia (flashes of light), and visual field defects with an enlarged blind spot. In fact, acute idiopathic blind spot enlargement (AIBSE) syndrome may be a late manifestation of MEWDS after a decrease or disappearance of the white dots (Hamed et al., 1988).

MEWDS is characterized by yellowish lesions in the deep retina, which can vary in size from small dots (<200 μm) to larger spots (≥200 μm) (Jampol et al., 1984). The dots tend to cluster around the optic disc or the vascular arcades, while the spots are more prominent in the mid-periphery (Pichi et al., 2016). A yellow stippled discoloration of the fovea, known as foveal granularity or Jampol dots (Onishi et al., 2019), mild disc edema, vascular sheathing, and vitreous cells may also be observed. Visual acuity varies significantly according to foveal involvement.

The retinal lesions in MEWDS are transient, and most patients experience spontaneous recovery. As a result, anti-inflammatory or immunosuppressive treatment is not recommended.

3.1.2. Pathogenesis

MEWDS primarily involves the outer retinal layers, and it is characterized by acute dysfunction of photoreceptors and RPE without choroidal perfusion defects. Recent studies utilizing adaptive optics scanning laser ophthalmoscopy (AOSLO) (Labriola et al., 2016; Onishi et al., 2019) and en-face OCT reconstructions (Pichi et al., 2016) have confirmed that MEWDS primarily affects the outer segments of photoreceptors, with relatively preserved inner segments. Advanced SD-OCT prototypes with higher axial resolution have suggested possible primary involvement of the IZ during the acute phase (Spaide and Lally, 2021).

It is still unknown whether the inflammation starts in the photoreceptors ("photoreceptoritis") or the RPE, but the initial electrophysiology findings and advanced retinal imaging supports the initial involvement of the photoreceptors with secondary RPE dysfunction (Onishi et al., 2019; Sieving et al., 1984; Spaide and Lally, 2021).

Sequential retinal imaging sometimes reveals a biphasic pattern of retinal inflammation, including a short phase of worsening of retinal lesions after the onset of symptoms. Outer retinal disruption usually begins in the fovea and around the optic disc, then extends toward the retinal periphery (Cahuzac et al., 2017; Hashimoto and Kishi, 2015). The histopathological explanation for the preference of MEWDS for peripapillary and foveal photoreceptors is currently unknown.

3.2. Imaging findings of MEWDS

3.2.1. OCT and OCTA features

Spectral-domain OCT in the active phase reveals multiple areas of attenuation in the ellipsoid zone/interdigitation zone (EZ/IZ), which correspond to the location of the white "spots" seen on clinical examination (Dell'omo et al., 2010b). In the early recovery phase, the disruption of the EZ gradually improves from diffuse to focal. In the late recovery phase, the EZ becomes continuous. Hyperreflective lesions of variable size are observed anterior to the spots. These lesions extend into the outer nuclear layer (ONL) or the outer plexiform layer (OPL) and correspond to the "dots" seen in other MMI techniques (Gal-Or et al., 2019; Pichi et al., 2016). The dots always appear over the spots and sometimes coalesce into linear extensions from the external limiting membrane (ELM) to the OPL. Additionally, a hyperreflective, ill-defined material, likely corresponding to degenerated outer segments, may be observed between the EZ and the RPE (Spaide and Lally, 2021) (Fig. 8).

Involvement of the fovea in MEWDS may result in RPE damage with choroidal hyper-transmission (Mantovani et al., 2019). Above the RPE, finger-like projections of hyperreflective material can extend from the IZ

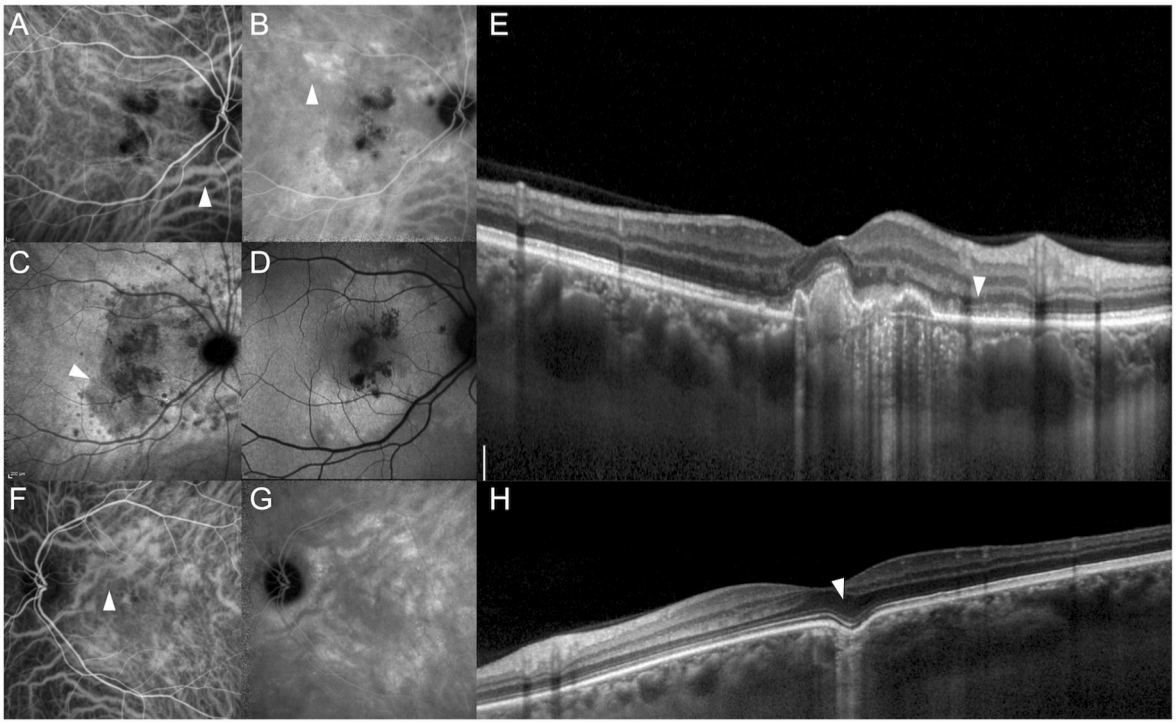

Fig. 6. Representative case of punctate inner choroidopathy/idiopathic multifocal choroiditis (PIC/iMFC) and secondary multiple evanescent white dot syndrome (MEWDS) in a patient with bilateral pachychoroid disease. Adapted from Ramtohul et al.
A. Early-phase indocyanine green angiography (ICGA) of the right eye reveals multiple hypofluorescent lesions consistent with PIC/iMFC (white arrowheads). Note the presence of dilated choroidal veins in the inferior macula (green arrowhead). B. Mid-phase ICGA of the right eye demonstrates multiple areas of choroidal vascular hyperpermeability (white arrowhead). C. Late-phase ICGA shows late hypofluorescent spots, partially confluent, surrounding the PIC/iMFC lesions (white arrowhead), suggestive of secondary MEWDS. D. Fundus autofluorescence imaging of the right eye displays multiple hypoautofluorescent lesions surrounded by hyperautofluorescence, suggesting secondary MEWDS. E. Optical coherence tomography (OCT) B-scan exhibits subretinal hyperreflective material splitting the retinal pigment epithelium/Bruch's membrane complex, associated with posterior signal hypertransmission and loss of the normal choroidal architecture. Additionally, diffuse increased choroidal thickness is observed in the macula, with pachyvessels compressing the inner choroid. Disruption of the ellipsoid zone and interdigitation zone near the PIC/iMFC lesions is also noted (white arrowheads), indicating secondary MEWDS. F. Early-phase ICGA of the left eye shows a discrete hypofluorescent lesion in the fovea. Additionally, dilated choroidal veins are observed in the superior macula (white arrowhead). G. Late-phase ICGA of the left eye reveals multiple areas of choroidal vascular hyperpermeability. H. OCT B-scan through the fovea demonstrates a conforming focal choroidal excavation (white arrowhead).

to the ONL or OPL. These lesions have been described as vertical intraretinal hyperreflective lines (Amoroso et al., 2021; Gal-Or et al., 2017; Mantovani et al., 2019), outer retinal plumes (Ramtohul et al., 2020), or foveal outer retinal hyperreflectivity (Dolz-Marco et al., 2021). These findings may not be necessarily visible on other imaging modalities.

The foveal outer retinal hyperreflectivity may be attributed to inflammatory cells, including microglia, and/or structural RPE damage. While all these hypotheses are plausible, the presence of vertical intraretinal hyperreflective lines may represent activated Müller cells and may correspond to a transient increase in hyperreflective dots observed on the retinal surface with en-face OCT reconstructions (Cicinelli et al., under review). Although no comparative studies have been conducted, foveal outer retinal hyperreflectivity has been associated with worse visual acuity and more severe functional scotoma on microperimetry (Dolz-Marco et al., 2021).

OCTA studies have not significantly contributed to the understanding of MEWDS but have confirmed normal choroidal and retinal perfusion in both the acute and subacute phases of the disease (Pichi et al., 2016).

3.2.2. FAF features

In MEWDS, the spots appear as indistinct areas of hyper-FAF on short-wavelength FAF (SW-FAF, 488 nm) or green-wavelength FAF (532 nm). This hyper-FAF results from the unmasked RPE FAF due to photoreceptor defects (Freund et al., 2013) (Fig. 9). Conversely, spots exhibit hypo-FAF on near-infrared FAF (NIR-FAF, 820 nm) due to the rearrangement of melanin-containing structures within the RPE (Battaglia Parodi et al., 2015; Mantovani et al., 2019; Zicarelli et al., 2020).

During the subacute phase of MEWDS, the spots typically resolve, but dotted hyper-FAF may appear on SW-FAF (Dell'Omo et al., 2010a; Gal-Or et al., 2019) (Figs. 9 and 10). The exact source of this dotted hyper-FAF is uncertain, but it may be associated with an increased amount of fluorophores, such as degenerated outer segment material, under the retina or within the RPE (Scharf et al., 2022).

3.2.3. FA and ICGA features

Fluorescein angiography may reveal early wreath-like hyperfluorescence with minimal staining, vascular leakage, and staining of the optic nerve. Wreath-like hyperfluorescence can result from choroidal transmission through photoreceptor or RPE defects, intraretinal microangiopathy, or activated microglia with a stellate configuration (Marsiglia et al., 2016).

Indocyanine green angiography demonstrates normal filling of the choroid and choriocapillaris. Spots become visible only in the middle to late phases as hypofluorescent lesions (Marsiglia et al., 2016), and new spots may emerge within hours after the examination (Zicarelli et al., 2020). The dots appear as darker punctate hypofluorescence in the deep retina, located anterior to the spots. While dots always colocalize with the spots, there can be areas that demonstrate spots with no evidence of dots.

The spots may merge to form large plaques around the posterior pole

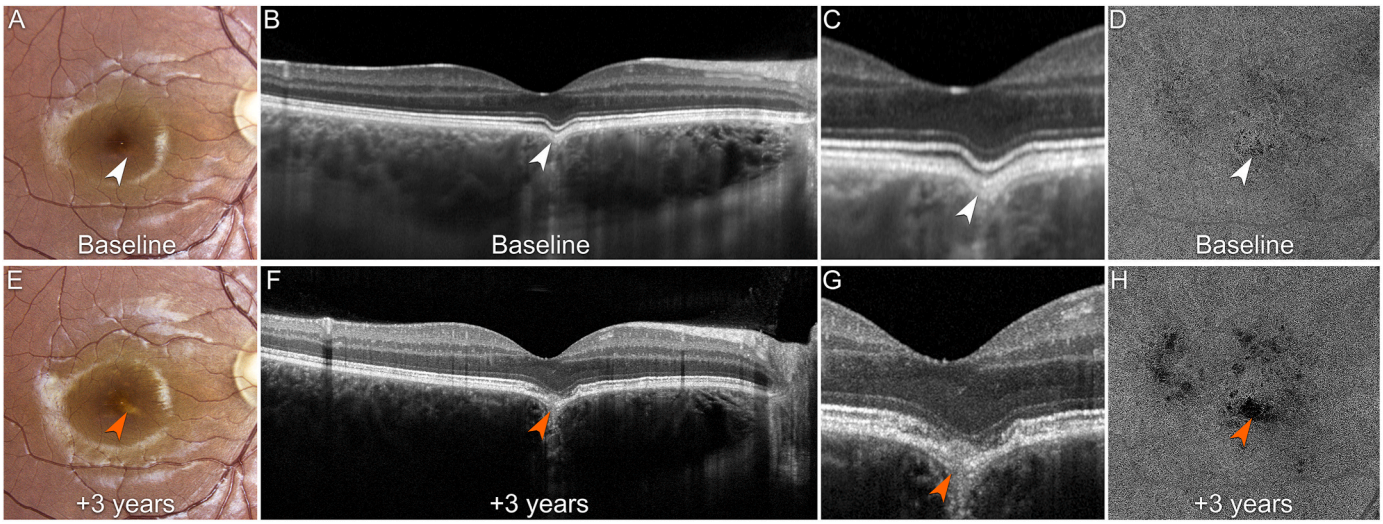

Fig. 7. Punctate inner pachychoroidopathy associated with pre-existent focal choroidal excavation and pachychoroid disease features.
A. Baseline confocal color fundus photography of the right eye reveals subtle hypopigmented changes of the retinal pigment epithelium (RPE) in the fovea (white arrowhead). The corresponding time point is displayed. B. Corresponding horizontal optical coherence tomography (OCT) B-scan through the fovea demonstrates a focal choroidal excavation (white arrowhead). Notably, there is diffuse increased choroidal thickness in the macula, with pachyvessels compressing the inner choroid. The corresponding time point is displayed. C. Magnified view of the focal choroidal excavation on SD-OCT (white arrowhead), highlighting the continuity of the ellipsoid zone (EZ). D. En-face swept-source OCT-angiography (SS-OCTA) segmented at the level of the choriocapillaris reveals subtle flow signal deficits (white arrowhead) colocalizing with the focal choroidal excavation. The corresponding time point is displayed. E. Three years later, confocal color fundus photography of the right eye displays a punctate inner choroidopathy (PIC) lesion (orange arrowhead). The corresponding time point is displayed. F. Horizontal high-resolution OCT (High-Res OCT) B-scan through the fovea illustrates a discrete subretinal hyperreflective material splitting the RPE/Bruch's membrane (RPE/BrM) complex at the site of the focal choroidal excavation (orange arrowhead). Additionally, there is posterior signal hypertransmission. The corresponding time point is displayed. G. Magnified view of the PIC lesion colocalizing with the focal choroidal excavation on High-Res OCT (orange arrowhead), showing disruption of the EZ band and focal RPE/BrM complex interruption. H. En-face SS-OCTA segmented at the level of the choriocapillaris displays an enlargement of the flow signal deficits colocalizing with the PIC lesion (orange arrowhead). The corresponding time point is displayed.

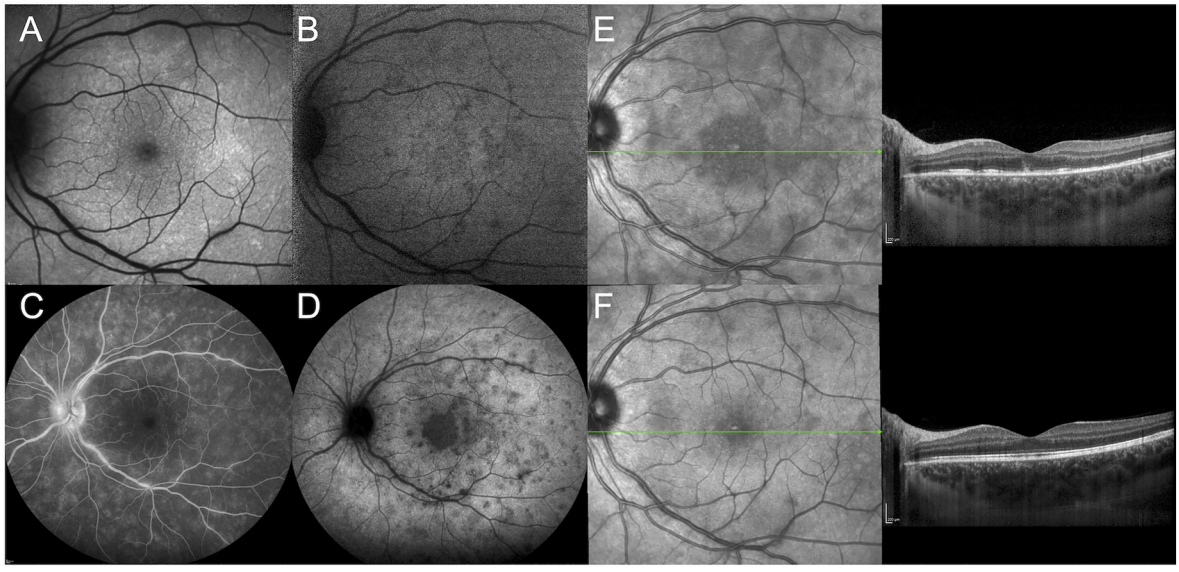

Fig. 8. Representative case of multiple evanescent white dot syndrome (MEWDS).
A. Short-wavelength fundus autofluorescence (SW-FAF, 488 nm) of the left eye reveals a large area of hyperautofluorescence in the posterior pole. B. Near-infrared FAF (NIR-FAF, 820 nm) displays hypoautofluorescence, likely due to rearrangement of melanin-containing structures within the retinal pigment epithelium (RPE). C. Fluorescein angiography exhibits wreath-like hyperfluorescence of the outer retinal lesions with minimal staining, vascular leakage, and staining of the optic nerve. D. Late phase of indocyanine green angiography demonstrates hypofluorescent dots and spot lesions within and outside the vascular arcades. E. Optical coherence tomography (OCT) B-scan shows multiple areas of attenuation in the ellipsoid and interdigitation zones (EZ/IZ). Additionally, there is a hyperreflective, ill-defined material at the fovea originating from the EZ and protruding into the outer nuclear layer. F. Follow-up OCT acquired 3 months later at the same location as in E reveals nearly complete restoration of the EZ/IZ band and disappearance of the hyperreflective material in the fovea.

(Gross et al., 2006; Marsiglia et al., 2016), which some authors hypothesized to possibly correspond to areas of reduced indocyanine green uptake by dysfunctional and inflamed RPE cells (Chang et al., 2005; Gaudric and Mrejen, 2017).

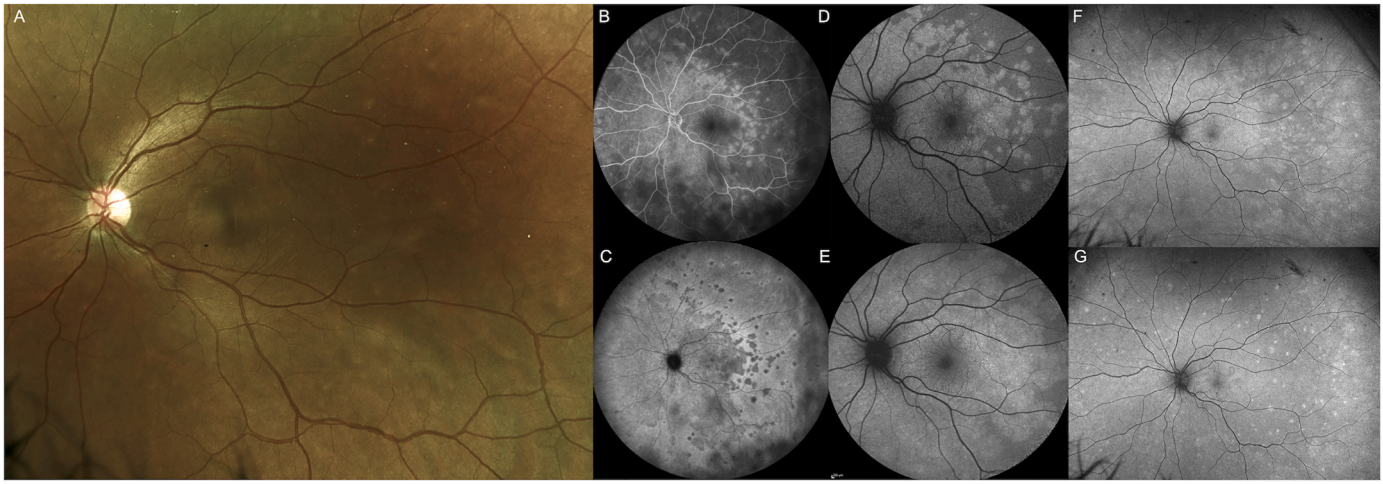

Fig. 9. Representative case of spontaneous resolution of multiple evanescent white dot syndrome (MEWDS).
A. Pseudocolor fundus photography of the left eye reveals yellowish lesions in the deep retina, more prominent in the mid-periphery. B. Fluorescein angiography displays wreath-like hyperfluorescence involving the entire posterior pole and extending toward the nasal periphery. C. Late phase of indocyanine green angiography demonstrates hypofluorescent dot and spot lesions within and outside the vascular arcades, along with a confluent plaque of hypofluorescence surrounding the optic nerve. D. Short-wavelength fundus autofluorescence (SW-FAF, 488 nm) in the acute phase shows confluent hyperautofluorescence in the same territory as the angiographic findings. E. SW-FAF imaging acquired 3 weeks after baseline demonstrates progressive resolution of the hyperautofluorescence and the appearance of dotted hyperautofluorescence temporally to the fovea. F-G. Green-wavelength FAF (532 nm) acquired at the same time points as D and E depict progressive normalization of the diffuse hyperautofluorescence and persistence of mid-peripheral dots.

3.2.4. Microperimetry

Microperimetry has been used to monitor patients with acute MEWDS. It has revealed a diffuse reduction in macular sensitivity, consistent with the disruption of photoreceptors observed on SD-OCT and the presence of hypofluorescent spots on ICGA. There is also a significant decrease in retinal sensitivity around the optic nerve, which corresponds to the enlargement of the blind spot in the visual field and poor fixation stability. Macular sensitivity improves within three months, starting from the foveal region and progressing outward centrifugally (Hamed et al., 1989; Li and Kishi, 2009) (Fig. 10).

3.2.5. Electroretinogram

During the acute stage of MEWDS, the electroretinogram (ERG) shows profoundly decreased rod, maximal, and cone responses in the affected eyes compared with the fellow eyes, suggesting diffuse impaired photoreceptor function (Li and Kishi, 2009). The early receptor potential (ERP) regeneration times are also abnormally prolonged, implying abnormal visual pigment regeneration. During recovery, the ERG and ERP amplitudes return to normal (Sieving et al., 1984). ERG studies showed that retinal involvement in MEWDS is more widespread than the lesions on MMI (dots and spots) and confirmed that MEWDS primarily affects the photoreceptors.

The multifocal electroretinogram (mfERG) provides a significant advantage in localizing areas of retinal dysfunction compared to conventional full-field ERG, which offers a global response of the entire retina. With mfERG, multiple areas of the macula can be simultaneously assessed, facilitating the identification of localized retinal abnormalities. In active MEWDS, mfERG demonstrates a blunted foveal peak compared to the unaffected fellow eye (Oh et al., 2001). The retinal function almost completely recovers in inactive disease, and first-order responses equal those of the asymptomatic fellow eye (Li and Kishi, 2009).

3.3. Unusual findings in MEWDS

In addition to the classic form of MEWDS, atypical cases have been described. While rare, MEWDS can manifest bilaterally, affecting both eyes simultaneously or sequentially (Aaberg et al., 1985; Bosello et al., 2022; Finn and Khurana, 2021; Veronese et al., 2018). Most cases of MEWDS are isolated; however, a report from Israel documented a cluster of seven patients who presented with acute MEWDS within three months (Gal-Or et al., 2017). MEWDS predominantly affects women aged 20–50 years, but it can also occur in younger patients (Ramakrishnan et al., 2021; Wang et al., 2022). However, it is extremely rare after the age of 50.

Some authors have reported additional findings, including transient peripapillary serous detachments, likely attributed to transient dysfunction of the RPE in reabsorbing retinal fluids (Chao et al., 2015), or foveal exudation with pre-existing choroidal venous congestion (Chen et al., 2017). Other cases of MEWDS have been described with exclusive foveal involvement, lacking the characteristic spots and dots observed on clinical examination and MMI(Shelsta et al., 2011).

Classic MEWDS lesions resolve within three months without leaving any permanent effects (Casalino et al., 2017). The spots tend to disappear earlier than the dots, which may take several weeks to vanish. Foveal granularity may persist as well (Bosello et al., 2022). In some cases, rapid resolution of fundus lesions has been observed (Yenerel et al., 2008). Some patients may experience persistent EZ/IZ defects on OCT, hypofluorescence on ICGA, or slower visual recovery, especially if they are young or present with worse visual acuity (Bosello et al., 2022). AOSLO may show persistent discontinuity of the photoreceptor matrix at 3 months, despite normalization of OCT findings (Labriola et al., 2016; Onishi et al., 2019).

Microperimetry shows progressive normalization of macular function, although the enlarged blind spot may not completely disappear. No specific baseline multimodal imaging features have been associated with visual outcomes or the clinical course (Bosello et al., 2022).

Recurrences of MEWDS are rarely seen and often exhibit features overlapping with those of the primary occurrence (Tsai et al., 1994). Complications such as CNV and irreversible damage to the outer retina have been rarely reported (Wyhinny et al., 1990). However, the authors believe that the pigmentary/atrophic changes sometimes seen in recurrent or atypical MEWDS might indicate overlap with other diseases, such as PIC/iMFC (see Paragraph 4.C) (Barile and Harmon, 2017; Chen et al., 2017).

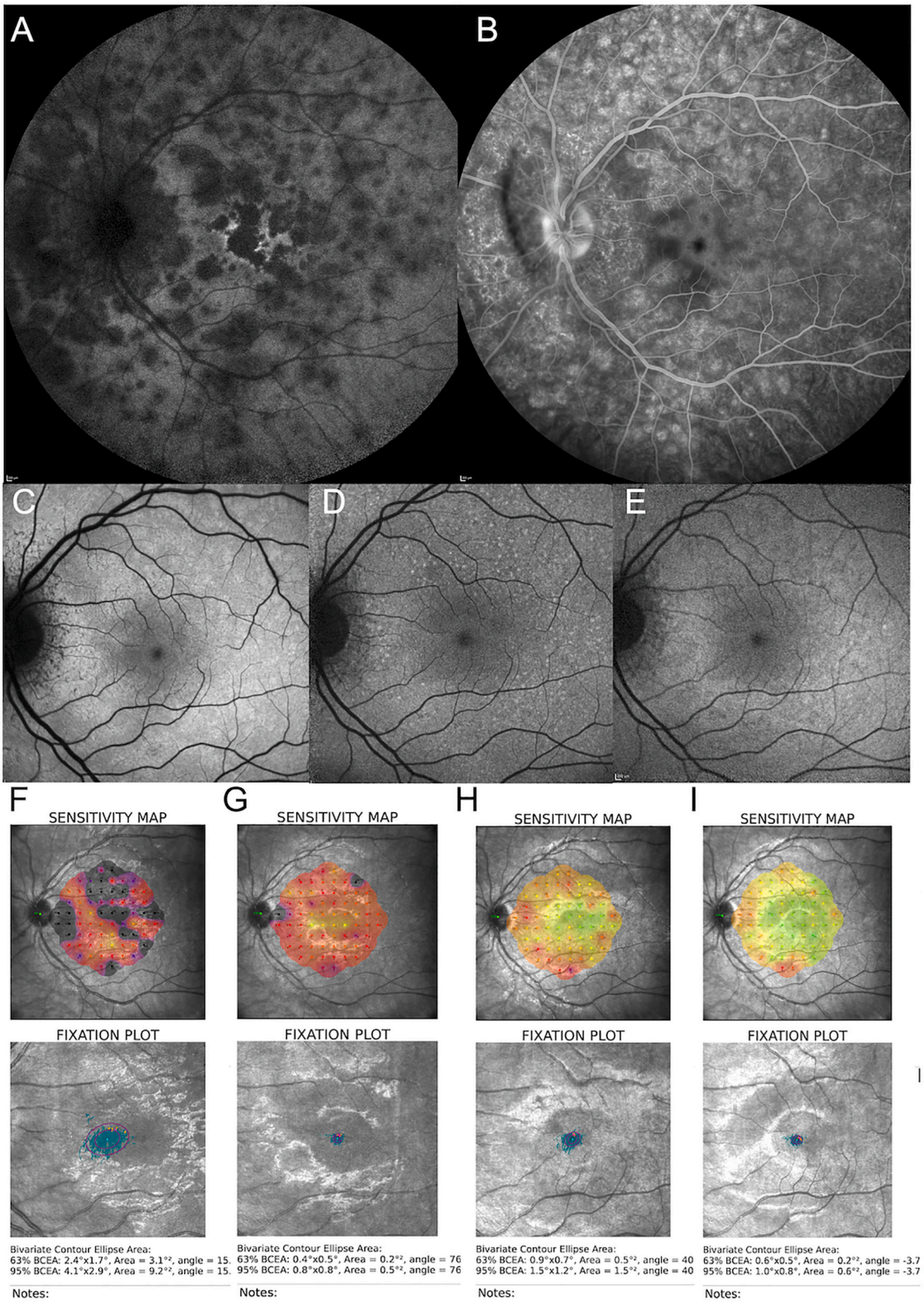

Fig. 10. Microperimetry in a patient with multiple evanescent white dot syndrome (MEWDS).
A. Late phase of indocyanine green angiography (ICGA) demonstrates hypofluorescent dot and spot lesions within and outside the vascular arcades, along with confluent hypofluorescence in the peripapillary area. B. Fluorescein angiography shows wreath-like hyperfluorescence, optic nerve staining, and leakage from large vessels. C. Short-wavelength fundus autofluorescence (SW-FAF, 488 nm) in the acute phase reveals diffuse hyperautofluorescence. D-E. SW-FAF imaging acquired 2 weeks (D) and 6 weeks (E) after baseline illustrates progressive resolution of the hyperautofluorescence and the appearance of dotted hyperautofluorescence. F. Microperimetry at baseline demonstrates a diffuse reduction in macular sensitivity, with areas of deeper relative scotoma colocalizing with the hypofluorescent spots on ICGA. There is also a decrease in retinal sensitivity around the optic nerve. G-I. Progressive normalization of macular sensitivity is observed. Additionally, there is a reduction in the fixation area, as indicated by the bivariate contour ellipse area.

4. Secondary WSS: PIC-like and MEWDS-like reactions

4.1. Acute retinopathy in PXE

Acute retinopathy with features of MEWDS has been described as a distinctive phenotype of outer retinal/RPE/BrM complex alterations occurring in patients with pseudoxanthoma elasticum (PXE) and angioid streaks (Gliem et al., 2019b). This condition is characterized by rapid vision loss and outer retinal whitish spots that appear hyperautofluorescent (Ramtohul et al., 2022a). Further characterization using high-resolution OCT has revealed two distinct phenotypes of outer retinal alterations: (1) hyperreflective dome-shaped lesions that split the RPE/BrM complex and associated with focal choroidal thickening, which later resolve with RPE/BrM atrophy, and (2) transient disruption of the EZ/IZ corresponding to zonal hyperautofluorescence that recovers completely (Fig. 11) (Ramtohul et al., 2022a).

The description of acute retinopathy in patients with PXE contributed to a re-interpretation of WSS and their pathogenesis, previously hypothesized by other authors (Bryan et al., 2002; Fung et al., 2012). The hypothesis of secondary WSS was first introduced. Subsequently, additional cases of secondary WSS (either presenting as PIC/iMFC or MEWDS) have been recognized and collectively described.

4.2. Secondary PIC/iMFC in unrelated chorioretinal disorders

Cicinelli et al. described active PIC/iMFC lesions in patients with unrelated chorioretinal diseases, including PXE, angioid streaks, autosomal recessive bestrophinopathy, rod-cone dystrophy, neovascular age-related macular degeneration, ocular trauma with chorioretinal rupture, rhegmatogenous retinal detachment, toxoplasmic chorioretinitis, and Stargardt disease. These PIC/iMFC lesions occurring in the context of unrelated chorioretinal disorders are referred to as secondary PIC (Cicinelli et al., 2022a). Secondary PIC/iMFC differs from primary PIC/iMFC in age, gender, laterality, prodromes, and refractive errors.

Clinically, the occurrence of secondary PIC/iMFC is characterized by acute or subacute vision decline. In cases with pre-existing chorioretinal scars, the detection of overlying PIC/iMFC lesions primarily relies on OCT imaging, which shows subretinal iso/hyperreflective material splitting the RPE/BrM complex, focal interruption and downward deflection of the BrM, and underlying choroidal thickening with loss of the normal vascular architecture.

Complications related to secondary PIC/iMFC may develop, leading to permanent vision loss, including punched-out chorioretinal scars, macular atrophy, subretinal fibrosis, Schlaegel lines, and CNV (Cicinelli et al., 2022a; Gliem et al., 2019b; Marchese et al., 2018a, 2018b). Recurrences of inflammation can also be observed (Ramtohul et al., 2022a). In recurrent or complicated cases, additional management may be necessary, such as corticosteroids, immunosuppressive therapies, and intravitreal injections of anti-VEGF agents.

4.3. Secondary MEWDS

While primary MEWDS occurs in otherwise healthy eyes, there have been increasing reports and series describing MEWDS associated with or subsequent to other chorioretinal diseases (Cicinelli et al., 2020a; Essilfie et al., 2022). These cases we now call secondary MEWDS. The terms MEWDS-like reactions (Cicinelli et al., 2020a) and epiphenomenon MEWDS (epi-MEWDS) (Essilfie et al., 2022) have also been used.

The most common associations with secondary MEWDS are listed in Table 1. It is important to note that in some cases where the term "secondary MEWDS" has been applied, there may have been concurrent secondary PIC/iMFC findings, and often these reactions exhibit overlapping features.

Secondary MEWDS may not begin simultaneously with the triggering disease but can be delayed days to years after the primary event (Fig. 12). Clinically, secondary MEWDS closely resembles cases of primary MEWDS and does not appear to affect the course of the associated disease (Essilfie et al., 2022). However, patients with secondary MEWDS tend to be older and have fewer and smaller spots on MMI (Fig. 13). Outer retinal disruption in secondary MEWDS typically initiates around the presumed triggering retinal lesion and gradually expands centrifugally, even after the initiation of immunosuppressive treatment for the primary disease (Abdelhakim et al., 2021).

Eyes with typical myopic degenerative findings can potentially develop secondary MEWDS and secondary PIC/iMFC changes. Notably, patients with secondary MEWDS and associated PIC/iMFC tend to have higher myopia (Meng et al., 2023). In secondary MEWDS, the distribution of lesions is often asymmetrical, both horizontally and vertically, with a preference for the retinal quadrant bearing the presumed chorioretinal trigger (Ong et al., 2023). The gender distribution, visual acuity at presentation, systemic and ocular symptoms, and choroidal thickness demonstrate the similarity between primary and secondary MEWDS (Serrar et al., 2022).

It is important to note that patients with pre-existing retinal diseases

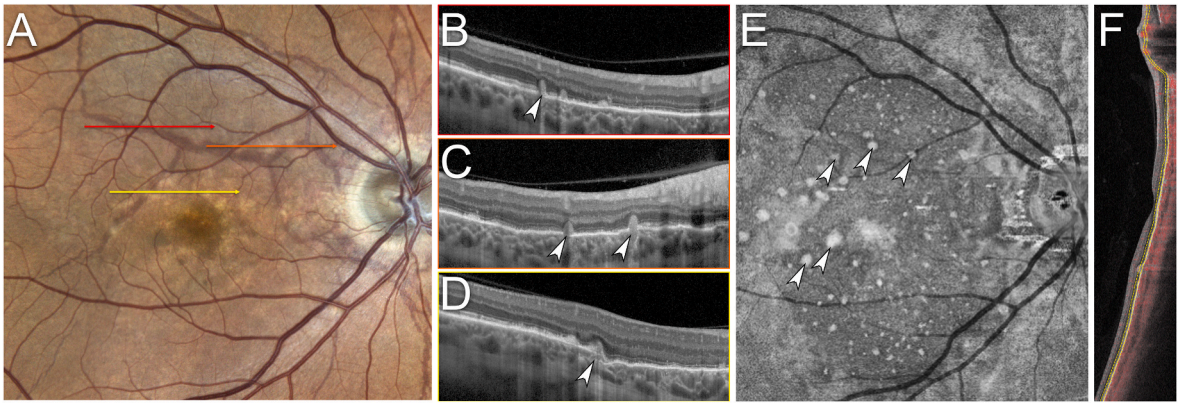

Fig. 11. Multimodal imaging of acute retinopathy in pseudoxanthoma elasticum. Adapted from Ramtohul et al.
A. Confocal color fundus photography of the right eye reveals multifocal, deep, yellowish lesions at the macula, with some lesions developing along angioid streaks (white arrowheads). The red, orange, and yellow lines indicate the location of the High-Resolution optical coherence tomography (High-Res OCT) B-scans displayed in panels (B), (C), and (D), respectively. B - D. High-Res OCT B-scans illustrate multiple hyperreflective, dome-shaped lesions that split the retinal pigment epithelium/Bruch's membrane complex (white arrowheads), accompanied by focal choroidal thickening, loss of the normal choroidal architecture, and posterior choroidal hypertransmission. These features are consistent with punctate inner choroidopathy/idiopathic multifocal choroiditis (PIC/iMFC) lesions. E-F. En-face widefield OCT displays multiple hyperreflective spots arranged in a splatter-like configuration (white arrowheads). The number of lesions observed on en-face widefield OCT exceeds those seen on fundus photography. The segmentation used is presented in panel (F).

Table 1
Diseases associated with secondary MEWDS.

	Reference
Other inflammatory diseases	
PIC/iMFC	(Battaglia Parodi et al., 2018; Bryan et al., 2002; Callanan and Gass, 1992; Kang et al., 2022; Meng et al., 2023; Serrar et al., 2022)
Ocular toxoplasmosis (acquired)	(Mabchour et al., 2023; Mathis et al., 2020; Serrar et al., 2022; Vance et al., 2011a)
Birdshot chorioretinopathy	(Cicinelli et al., 2022b; Serrar et al., 2022)
Optic neuritis on multiple sclerosis	Serrar et al. (2022)
AZOOR	Fine et al. (2009)
Ocular trauma or surgery	
Traumatic subretinal hemorrhage	Fung et al. (2012)
Retinal detachment	(Cicinelli et al., 2020a; Essilfie et al., 2022; Serrar et al., 2022)
Cryotherapy on peripheral retina	Serrar et al. (2022)
Thermal laser treatment to retinal tears	Golshani et al. (2020)
Radiotherapy to treat retinoblastoma	Serrar et al. (2022)
Acquired abnormalities	
Idiopathic atrophic scar	Serrar et al. (2022)
Angioid streaks (idiopathic or secondary to systemic diseases)	(Cicinelli et al., 2020a; Gliem et al., 2019a; Pece et al., 2016)
Choroidal neovascularization	(Mathis et al., 2018; Ong et al., 2023; Papadia and Herbort, 2010; Serrar et al., 2022)
Age-related macular degeneration	Cicinelli et al. (2022a)
Acute macular neuroretinopathy	Gass and Hamed (1989)
Central serous chorioretinopathy	Ong et al. (2023)
Congenital abnormalities or hereditary diseases	
Optic nerve coloboma	Serrar et al. (2022)
Ocular toxoplasmosis (congenital)	(Mathis et al., 2018; Serrar et al., 2022)
Best disease	(Bryan et al., 2002; Cicinelli et al., 2020a; Park et al., 1997; Serrar et al., 2022)

and secondary MEWDS may not recover visual function to the same extent as individuals with primary MEWDS in otherwise healthy eyes. Therefore, screening patients with active MEWDS for possible concurrent retinal conditions is crucial to rule them out. Recurrences of secondary MEWDS are rare and may be observed in conjunction with a relapse of the underlying disease, such as PIC/iMFC.

4.4. Common interpretation of secondary WSS

Secondary WSS are believed to be a possible immune-mediated response against retinal or inner choroidal antigens in the presence of two factors: 1) permissive host genetic susceptibility and demographic characteristics, and 2) immunogenic triggers. The permissive host genetic susceptibility may be the same as in primary WSS(Pearlman et al., 2009), although this is currently unknown.

Systemic infections (Jain et al., 2022; Miyata et al., 2022; Wiley et al., 2022), vaccinations (Ng et al., 2020; Yang et al., 2019), and stress are possible external immunogenic triggers associated with secondary WSS. The proposed link between infections and retinal or choroidal inflammation is the dysregulation of the host immune system. Similar risk factors have been observed in cases of WSS recurrence. Reports of WSS associated with vaccinations have increased after the COVID-19 outbreak, with over 25 cases of WSS described following COVID-19 vaccination (Seong and Lee, 2022; Soifer et al., 2022). While some of these cases may be coincidental, molecular mimicry due to structural similarities between human proteins and vaccine components, resulting in the creation of self-antigens, could be a plausible explanation (Jampol et al., 2021).

The outer retina is considered an immune-privileged space. Almost all reported cases of secondary WSS exhibited damage to the choriocapillaris, BrM, or RPE, along with compromise of the posterior retinal-

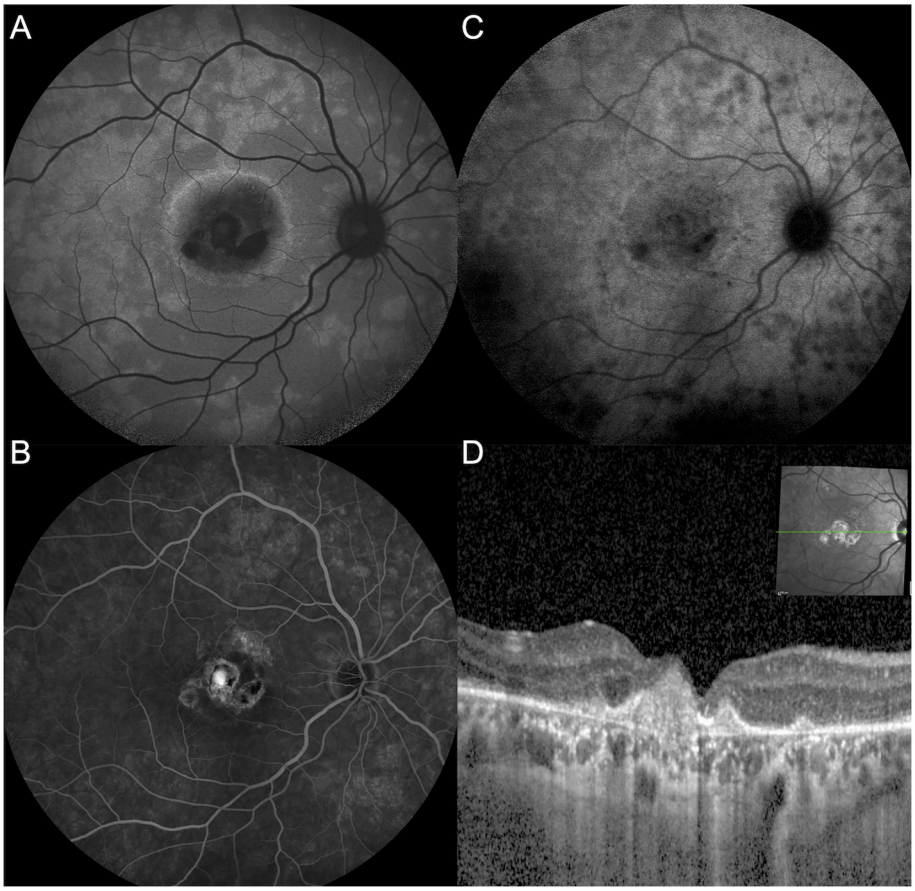

Fig. 12. Punctate inner choroidopathy and secondary multiple evanescent white dot syndrome (MEWDS). A. Fundus autofluorescence (FAF) imaging reveals multiple hypoautofluorescent lesions in the posterior pole, indicating retinal pigment epithelium (RPE) atrophy. There is a circular area of less defined hypo-FAF surrounded by a hyperautofluorescence ring. Confluent areas of hyper-FAF in the mid-periphery are suggestive of secondary MEWDS. B. Fluorescein angiography displays areas of early hyperfluorescence in the posterior pole, indicative of a window defect. There is active leakage observed in the macula. The hyperautofluorescent spots seen on FAF correspond to wreath-like hyperfluorescence outside the vascular arcades. C. Late-phase indocyanine green angiography showcases markedly hypofluorescent lesions in the macula, indicating choroidal inflammatory infiltration. Smaller hypofluorescent dots surrounding the macular lesions and ill-defined spots in the periphery are suggestive of secondary MEWDS. D. Optical coherence tomography B-scan demonstrates inner retinal thinning and a subretinal hyperreflective material between the retinal pigment epithelium and the Bruch's membrane. This is associated with posterior signal hypertransmission. The disruption of the ellipsoid zone and interdigitation zone near the punctate inner choroidopathy (PIC) lesions is visible.

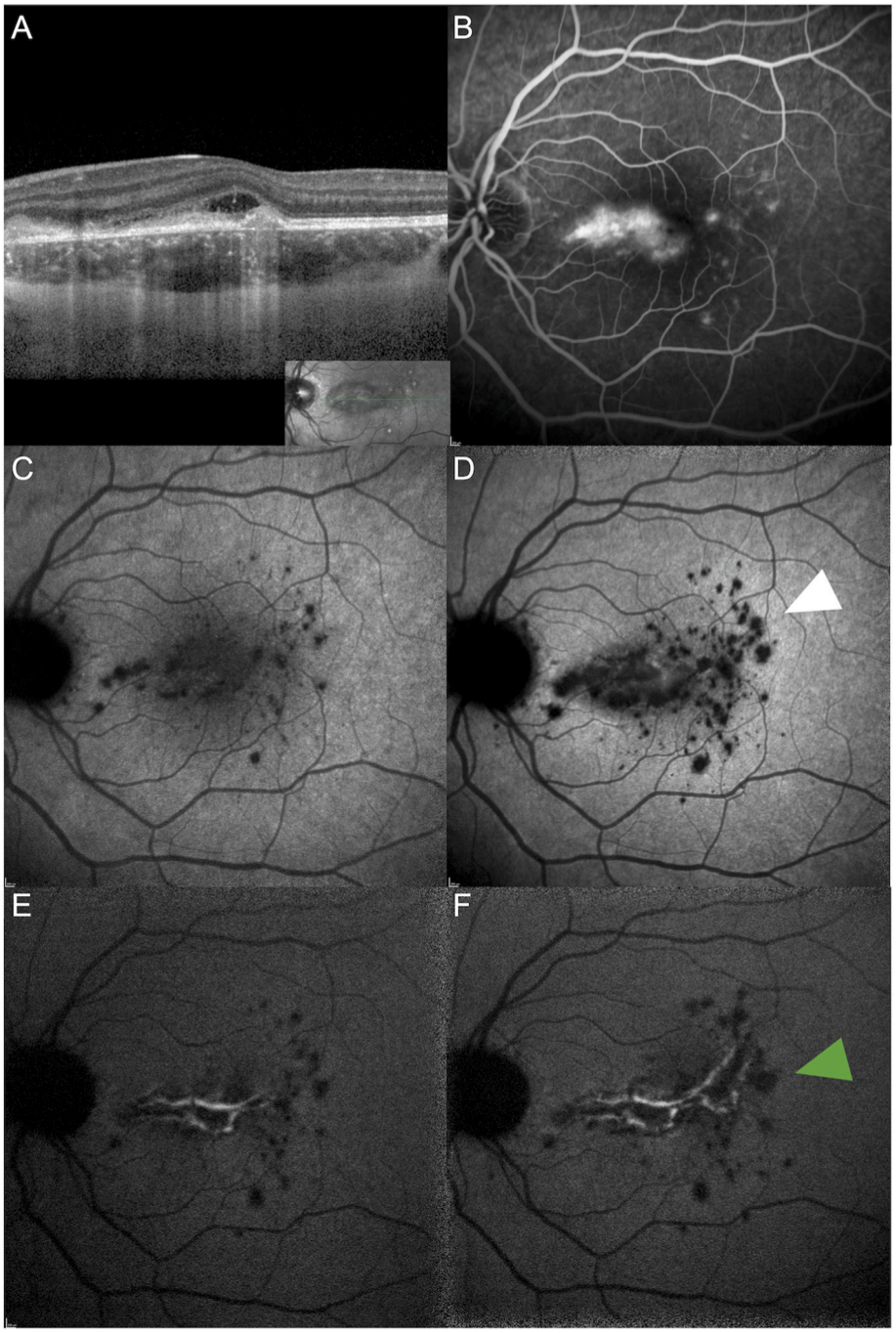

Fig. 13. Punctate inner choroidopathy and secondary multiple evanescent white dot syndrome (MEWDS) complicated by choroidal neovascularization (CNV).
A. Optical coherence tomography (OCT) B-scan reveals the presence of subretinal fluid and a hyperreflective material splitting the retinal pigment epithelium and the Bruch's membrane. This is associated with posterior signal hypertransmission. The interruption of the ellipsoid zone and interdigitation zone is observed. B. Fluorescein angiography demonstrates areas of hyperfluorescence in the posterior pole, indicating active leakage. Smaller wreath-like lesions temporally to the macula are also visible. C. Early phase of indocyanine green angiography (ICGA) displays multiple hypofluorescent lesions consistent with punctate inner choroidopathy. D. Late-phase ICGA reveals new hypofluorescent spots that were not observed in the early-phase ICGA, suggesting secondary MEWDS (white arrow). E. Near-infrared fundus autofluorescence (NIR-FAF, 820 nm) imaging illustrates a neovascular network corresponding to the area of leakage observed on fluorescein angiography. There are also hypo-FAF spots surrounding the CNV, colocalizing with the hypofluorescent spots observed on ICGA. F. Follow-up NIR-FAF imaging demonstrates an increase in the size of the CNV and an enlargement of the hypo-FAF spots surrounding the CNV (green arrow).

blood barrier. Exposure to new retinal antigens that are usually concealed from the immune system can lead to an autoimmune attack to the outer retina, clinically presenting as WSS (Cicinelli et al., 2020a; Essilfie et al., 2022) (Fig. 14). It is worth noting that many cases of secondary WSS have been observed in eyes with CNV, suggesting that the leaky vessels of CNV may contribute to maintaining outer retinal inflammation (Mathis et al., 2018).

The reasons why some patients present with secondary MEWDS while others develop secondary PIC/iMFC are unclear. Possible factors may include the target of the inflammatory insult (e.g., the photoreceptors, the RPE/BrM complex, or the inner choroid) or the type of antigen that initiates the inflammatory response. Similarly, the genetic and environmental factors predisposing individuals to secondary MEWDS or PIC/iMFC have not been determined. The authors have observed that most patients with secondary PIC/iMFC also have secondary MEWDS, suggesting a shared predisposition and indicating that they may be manifestations of similar immune system activation.

The natural history and therapeutic response of secondary WSS can differ. In the reported series, resolution of secondary PIC/iMFC was characterized by anatomical sequelae such as disruption of the outer retina and RPE/BrM complex. Further complications included macular atrophy and subretinal fibrosis. Although the available data are retrospective and have a relatively short follow-up period, eyes with secondary PIC/iMFC appeared to have a more destructive clinical course than those with secondary MEWDS. Therefore, we suggest that secondary PIC/iMFC should be treated (Cicinelli et al., 2022a). Considering the assumption of an autoimmune process, corticosteroid therapy may be considered in addition to treating the primary disease or concurrent

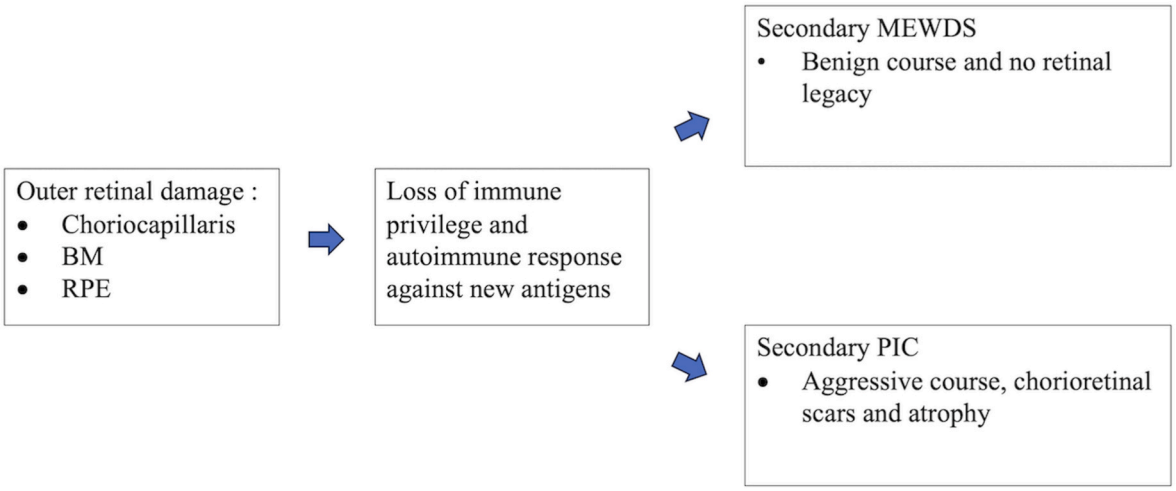

Fig. 14. Proposed pathogenesis of secondary white spot syndromes.
This diagram illustrates the hypothesized pathogenesis of secondary white spot syndromes, highlighting the key mechanisms involved in the development of these conditions. BM: Bruch's membrane; RPE: retinal pigment epithelium; MEWDS: multiple evanescent white dot syndrome; PIC: punctate inner choroidopathy.

complications such as CNV. Additional clinical observations are needed to establish therapeutic recommendations.

5. AZOOR

5.1. Background

5.1.1. Historical background

AZOOR was first described by Gass in 1993 when he reported on 13 patients experiencing rapid vision loss in one or more zones of their visual field, along with photopsia, minimal fundoscopic changes, and abnormal electroretinography affecting one or both eyes (Gass, 1993). Most of these patients were young women, and some had evidence of autoimmune diseases. Despite extensive medical and neurological evaluations, no associated findings were identified, and effective treatment remained elusive. During long-term follow-up, more than half of the eyes in AZOOR patients showed a normal fundus on the final examination, and only a minority exhibited progressive visual field loss (Gass et al., 2002). Rarely, AZOOR patients can be complicated by CNV (Introini et al., 2018).

Currently, no definitive treatment for AZOOR has been established that consistently improves visual outcomes. While systemic corticosteroids have been used with varying success (Gass et al., 2002; Monson and Smith, 2011), intravitreal injections of sustained-release corticosteroid devices have shown promise in inactivating the active edge in AZOOR (Vadboncoeur et al., 2022). Antivirals and systemic immunosuppressants have also been employed with mixed results (Lin et al., 2022; Mahajan and Stone, 2010; Monson and Smith, 2011).

5.1.2. Terminology

Regarding terminology, Gass suggested that AZOOR might belong to a broader spectrum of diseases sharing overlapping features, including MEWDS, AIBSE syndrome, and acute macular neuroretinopathy (AMN). However, the lack of a specific fundus biomarker has made it challenging to precisely define AZOOR, leading to heterogeneity in the cases described in the literature. Consequently, AZOOR has become a broad diagnostic term for chorioretinal diseases with visual loss of uncertain origin.

To refine the diagnosis of AZOOR based on MMI findings, Mrejen et al. proposed a novel classification relying on the identification of striking, progressive retinal changes involving outer retinal, RPE, and choroidal degeneration (Mrejen et al., 2014). Still, a subgroup of patients with consistent characteristics could be identified in the series from Mrejen et al. (see Paragraph 5.D).

5.2. Imaging findings of AZOOR

5.2.1. Clinical features of AZOOR according to the definition by Gass

In the cohort described by Gass et al., AZOOR initially presented as unilateral in 60% of the cases. Over an 8-year follow-up, bilateral involvement occurred in 76% of the patients after a median of 31 months, and one-third experienced recurrences (Gass et al., 2002). Visual acuity was 20/40 or better in at least one eye in 88% of the patients at the final visit.

At presentation, the fundus examination was normal in 90% of the cases. Within the early weeks after the onset of AZOOR, patients developed cystoid macular edema, perivenous exudation, multifocal chorioretinal scars, narrowed retinal vessels, and RPE atrophy and clumping resembling retinitis pigmentosa (Gass, 1993) (Fig. 15).

Subsequently, several groups described the MMI characteristics of "classic" AZOOR. Patients with AZOOR exhibit outer retinal thinning, EZ/IZ loss, and RPE irregularities on OCT (Li and Kishi, 2007). Fundus autofluorescence shows diffuse hyper-FAF or coarse granular regions of mixed hyper- and hypo-FAF (Wang et al., 2017). In some eyes, a well-defined hyper-FAF border is noted, associated with loss of the EZ band and a transition from relatively normal to markedly decreased or non-recordable visual sensitivity on microperimetry testing (Duncker et al., 2018; Fujiwara et al., 2010; Wang et al., 2017).

Fluorescein angiography reveals window defects or blockage related to RPE changes, retinal vascular staining or leakage, diffuse intraretinal staining, cystoid macular edema, optic disc staining, and peripheral hyperfluorescent spots (Monson and Smith, 2011). Indocyanine green angiography has been investigated in a few studies and shows normal choroidal fluorescence in patients with no RPE changes and hypofluorescence in cases involving RPE (Spaide, 2004). AOSLO frequently reveals cone loss with increased spacing in the regions corresponding to EZ/IZ abnormalities and visual field loss (Merino et al., 2011; Mkrtchyan et al., 2012; Xu et al., 2022). Although it is still unclear which level of photoreceptor AOSLO does image, the abnormal cone reflectivity in AOSLO might indicate dysfunction of mitochondria cone inner segment ellipsoids (Nakao et al., 2015). These changes may normalize upon follow-up (Nakao et al., 2015).

Automated static threshold perimetry documents one or more zones of visual field loss, and there is evidence of generalized dysfunction on electrooculogram and ERG (Francis et al., 2005).

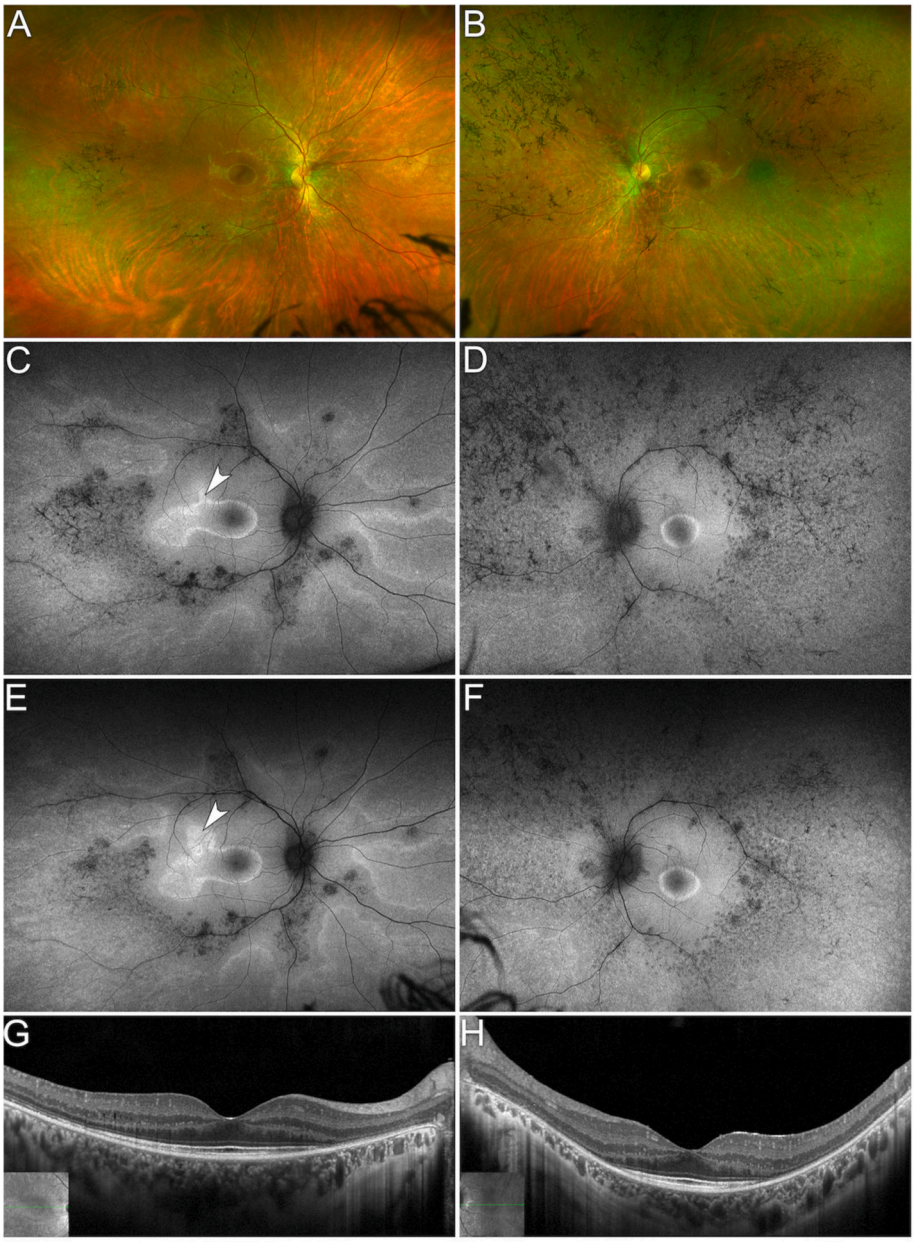

Fig. 15. Multimodal imaging of a case of acute zonal occult outer retinopathy (AZOOR) according to the definition by Gass and Stern.
A woman in her 20s presented with rapid visual field loss and photopsia in both eyes at the age of 14. She noted stabilization of her visual symptoms under methotrexate 2.5 mg/day. Panel-based genetic testing was negative. Her visual acuity was 20/20 in both eyes. A-B. Ultra-widefield pseudocolor fundus photography of the right (A) and left eye (B) shows degeneration of the retinal pigment epithelium (RPE) around the optic disc, along the vascular arcades, and in the mid-periphery. C-D. Ultra-widefield fundus autofluorescence imaging of the right (C) and left eye (D) shows diffuse hypoautofluorescent zones corresponding to RPE and photoreceptor loss. Note the hyperautofluorescent area in the perifoveal region of the right eye corresponding to photoreceptor loss and relatively preserved RPE (*white arrowhead*). E-F. At the 5-year follow-up, ultra-widefield fundus autofluorescence imaging of the right (E) and left eye (F) shows progression of the hyperautofluorescent zone in the perifoveal region of the right eye (*white arrowhead*) which corresponds to photoreceptor loss and recent visual field constriction. Note the relative stability of the autofluorescent anomalies in the left eye. G-H. High-resolution optical coherence tomography of the right (G) and left eye (H). In the right eye (G), the B-scan shows ellipsoid (EZ) and interdigitation zone (IZ) disruption in the temporal side of the fovea, which colocalizes with hyperautofluorescent lesion on ultra-widefield fundus autofluorescence imaging. In the left eye (H), preservation of the foveal EZ/IZ is noted. The insets are the near infrared reflectance images with the green line indicating the position of the B-scans.

5.2.2. *Clinical features of AZOOR according to the definition by Mrejen et al*

Mrejen et al. conducted a study with 30 AZOOR patients who initially presented with photopsia and scotoma, with most of them exhibiting detectable fundus changes. On fundoscopic examination, patients in the early phase of AZOOR showed a transient white line at the margin of the involved zone, which displayed a granular hyper-FAF signal. Additionally, these patients had a patchy hyper-FAF signal and diffuse photoreceptor loss on OCT (Mrejen et al., 2014).

Patients in more advanced stages of AZOOR exhibited zonal areas of outer retinal, RPE, and choroidal degeneration surrounded by a grey/orange demarcating line that appeared continuous, interrupted, or scalloped on fundus exam. The peripapillary region was the most frequently involved, but some patients presented with satellite skip lesions in the mid- and far-periphery. AZOOR lesions exhibited a characteristic "trizonal pattern," where zone 1 represented areas with intact retinal and RPE layers, zone 2 corresponded to the demarcation line between affected and unaffected areas, and zone 3 corresponded to areas of outer retina and RPE atrophy that directly aligned with the AZOOR lesion (Mrejen et al., 2014) (Fig. 16). On OCT, zone 1 showed normal retinal and choroidal layers, zone 2 exhibited multifocal subretinal mound-like hyper-reflective material, and zone 3 displayed EZ/IZ disruption, RPE atrophy, and choroidal thinning. Fundus autofluorescence also demonstrated a trizonal pattern, including normal FAF signal in zone 1, speckled hyper-FAF in zone 2, and hypo-FAF in zone 3.

AZOOR lesions tended to enlarge over time, extending towards the macula and the periphery. Central lesions tended to merge with skip lesions, encompassing almost all of the fundus. The pattern of lesion enlargement was usually not continuous but rather episodic, characterized by long periods of stability and short periods of progression. Notably, the persistence of the demarcation line was invariably associated with disease progression (Table 2).

Mrejen et al. highlighted the "trizonal pattern" and the progressive nature of the lesions as defining MMI features of AZOOR.

5.2.3. *Acute annular outer retinopathy*

In 1995, Gass and Stern reported a case of a 23-year-old man who presented with an acute scotoma in one eye, accompanied by a deep

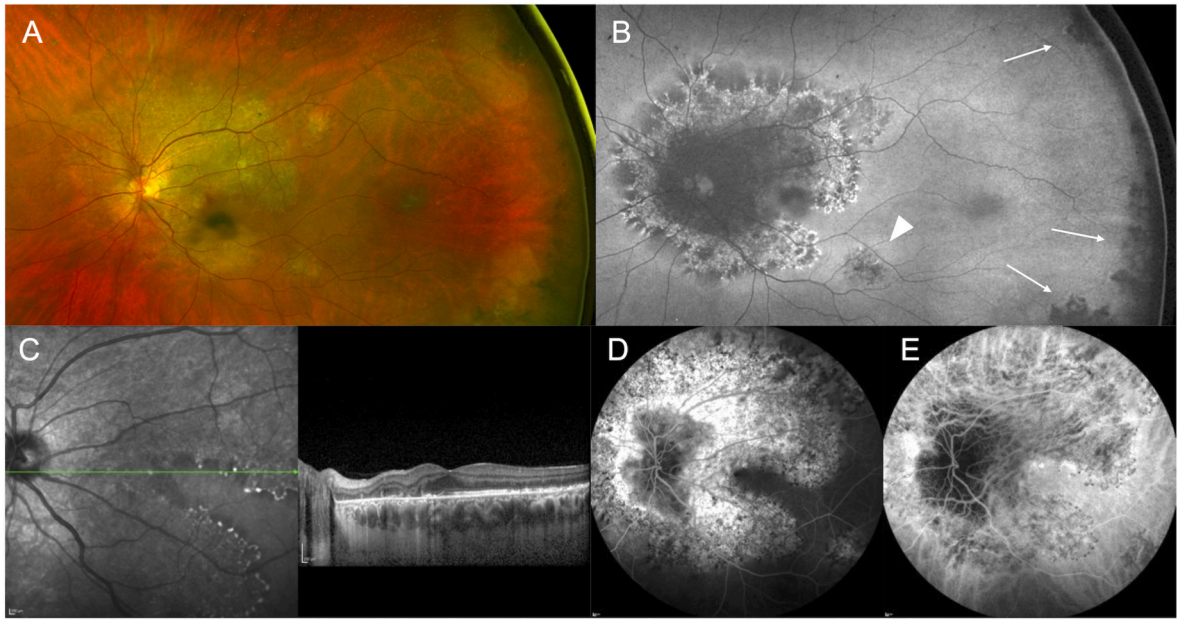

Fig. 16. Multimodal imaging of acute zonal occult outer retinopathy (AZOOR) according to Mrejen et al. This case shows features compatible with a distinct disease called "Multizonal Outer Retinopathy and Retinal Pigment Epitheliopathy" (MORR), a subtype of AZOOR or a novel clinical entity.
A. Pseudocolor fundus photography demonstrates degeneration of the retinal pigment epithelium (RPE) around the optic disc, along the vascular arcades, in the mid-periphery, and at the ora serrata. B. Fundus autofluorescence (FAF) imaging displays a peripapillary area of hypoautofluorescence surrounded by speckled hyper-FAF. An isolated lesion (indicated by a white arrowhead) and peripheral lesions (indicated by arrows) are also visible. C. Optical coherence tomography (OCT) B-scan reveals areas of outer retina and RPE atrophy nasally, while the outer retina appears intact around the fovea. Temporally, irregularities and clumping of the RPE are observed. D. Fluorescein angiography highlights a window defect at the core of the peripapillary lesion and irregular blockage at the demarcation line. E. Indocyanine green angiography reveals mild hypofluorescence of the peripapillary lesion, suggesting possible loss of choriocapillaris perfusion and reduced uptake by the RPE.

Table 2
Stages of AZOOR as proposed by Mrejen et al. [adapted from Mrejen S, Khan S, Gallego-Pinazo R, Jampol LM, Yannuzzi LA. Acute zonal occult outer retinopathy: a classification based on multimodal imaging. JAMA Ophthalmol. 2014 Sep; 132 (9):1089–98. https://doi.org/10.1001/jamaophthalmol.2014.1683. PMID: 24945598.].

	Early	Intermediate	Late
Fundus appearance	Often normal	Atrophy of retina, RPE, and choroid (often peripapillary) surrounded by a yellow/orange line	Extensive retinal, RPE, and choroidal atrophy
	White or grey ring (Acute annular outer retinopathy)	Skip lesions in the mid- and far-periphery	No demarcation line Bone spicule pigmentation
FAF	Diffuse patchy hyper-FAF	Trizonal pattern: 1. Normal periphery	Trizonal pattern or diffuse hypo-FAF
	Ring of granular hyper-FAF signal	2. Speckled hyper-FAF 3. Central confluent hypo-FAF	No demarcation line
Spectral-Domain Optical Coherence Tomography	EZ/IZ disruption	Trizonal pattern: 1. Normal retinal and choroidal layers	Extensive retinal, RPE, and choroidal atrophy
	Focal thickening and hyperreflectivity of the outer nuclear layer and the Henle fiber layer	2. Multifocal subretinal mound-like hyperreflective material 3. EZ/IZ disruption, RPE atrophy, and choroidal thinning	Possibly inner retinal atrophy

EZ/IZ: ellipsoid and interdigitation zone; FAF: fundus autofluorescence; RPE: retinal pigment epithelium.

grey retinal ring corresponding to the margin of the scotoma (Gass and Stern, 1995). Based on its clinical characteristics, he named this condition acute annular outer retinopathy (AAOR). The ring progressively enlarged over weeks and eventually disappeared. Within the area where the ring was visible, gradual depigmentation of the fundus and pigmentary changes occurred.

Similar cases with comparable features were described (Fekrat et al., 2000; Liu et al., 2021; Seetharam et al., 2015). Seetharam et al. demonstrated that the transient subretinal ring observed in these cases corresponded to thickening and hyperreflectivity of the ONL and the Henle fiber layer on OCT. Recently, Ramtohul et al. proposed the term "angular sign of Henle fiber layer hyperreflectivity" to describe this OCT feature and suggested that an acute insult to the whole photoreceptor cell compartments (from the synapses to the outer segments) may be involved early in the course of acute annular outer retinopathy (Ramtohul et al., 2022b). When the disease subsided, outer retinal atrophy developed (Seetharam et al., 2015).

Although AAOR could represent a variant of AZOOR (Gass and Stern, 1995), the latest interpretation suggests it may be cases of AZOOR in which the delineation line is acutely apparent ophthalmoscopically as a white or grey line. This white line fades but can be replaced by a delineating orange line (Mrejen et al., 2014).

5.3. *Differential diagnosis of AZOOR*

Since its initial description, significant heterogeneity has become apparent in AZOOR, with variations in clinical appearance, natural progression, and treatment response (Mrejen et al., 2014).

Distinguishing AZOOR from other conditions that present with similar symptoms and clinical features, such as iMFC with outer retinal atrophy, autoimmune retinopathies, inherited retinal dystrophies, and infectious diseases like syphilis or tuberculosis, can be challenging, particularly in settings where MMI techniques and genetic testing are not readily available.

Ultra-widefield fundus color and FAF imaging can be particularly valuable in distinguishing AZOOR from inherited retinal dystrophies (Cicinelli et al., 2020b). Conditions such as ROSAH syndrome (retinal dystrophy, optic nerve edema, splenomegaly, anhidrosis, and headache), autosomal dominant vitreoretinochoroidopathy, RP1L1-related macular dystrophy, and CRB1-related dystrophies may share certain features with AZOOR, such as peripapillary involvement and progressive outer retinal atrophy (Bujakowska et al., 2012; Lafaut et al., 2001; Williams et al., 2019). However, each of these entities possesses distinct clinical characteristics, and a definitive genetic diagnosis can be established through appropriate testing.

Autoimmune retinopathy is another acquired condition that enters the differential diagnosis for AZOOR, encompassing various diseases, some of which are associated with neoplastic disorders. Autoimmune retinopathies are characterized by a more widespread outer retinal loss at presentation compared to AZOOR, and a few specific anti-retinal antibodies, such as anti-23-kDa-recoverin (Dutta Majumder et al., 2020) and alpha-enolase (Grewal et al., 2014). Finally, posterior uveitis and placoid chorioretinopathies involving the RPE and the outer retina can also mimic AZOOR, and the initial assessment should include a work-up for syphilis and tuberculosis to exclude these conditions (Marchese et al., 2022a).

5.4. Novel interpretations of AZOOR: multi-zonal outer retinopathy and retinal pigment epitheliopathy

The availability of MMI, including ultra-widefield imaging and long-term follow-up, has prompted a reevaluation of the definition of AZOOR. Notably, a subgroup of the patients included in the series from Mrejen et al. exhibited characteristics that contrasted with the initial description by Gass et al. (Gass, 1993).

Key differences were:

- Initial bilateral involvement, in contrast to the predominantly unilateral involvement in Gass' first description.
- Relentless expansion of lesions, compared to stable disease often seen in "classic" AZOOR.
- Involvement of multiple areas of the retina (peripapillary area, mid-periphery, far-periphery, or the macula) instead of discrete zonal areas of outer retinal changes.
- Clearly visible lesions on ophthalmoscopy or MMI, as opposed to occult lesions in AZOOR.
- Predominant RPE involvement, in contrast to Gass' hypothesis that AZOOR primarily affects the photoreceptors.
- Absence of optic disc edema, perivascular exudation, vascular sheathing, or vitritis, unlike the detection of these features in the long-term follow-up (Gass et al., 2002).
- No bone spicule pigmentation or retinal vascular narrowing resembling retinitis pigmentosa.
- Stereotypical natural course involving far-peripheral lesions with centripetal progression.
- Possible response to intravitreal corticosteroids with partial regression of the peripapillary lesion in contrast to no discernible improvement after administration of corticosteroids in Gass' patients (Gass et al., 2002).

These striking discrepancies have led the authors of this review to hypothesize that these patients could represent a distinct phenotype, and the eponym "Multizonal Outer Retinopathy and Retinal Pigment Epitheliopathy" (MORR) has been proposed (Fig. 17) (Ramtohul et al., under review). Other groups have reported cases with features potentially consistent with MORR (Boudreault et al., 2017; Hoang et al., 2013b; Introini et al., 2018; Lin et al., 2022; Makino et al., 2013; Marchese et al., 2020; Spaide, 2004; Vadboncoeur et al., 2022).

Like AZOOR, the etiology of MORR remains unknown, and prior speculations for AZOOR, including infectious, genetic, and autoimmune causes, also remain valid for MORR (Gass et al., 2002). The recognition of MORR as a separate entity may help reduce the heterogeneity in AZOOR patients and facilitate exploring potential treatment strategies, including long-lasting intravitreal corticosteroids.

6. Conclusion and future directions

White spot syndromes represent a diverse group of retinal disorders characterized by white or yellow lesions on fundus examination and involvement of the outer retina and inner choroid. The utilization of various imaging techniques has demonstrated the unique patterns of lesion distribution and progression within these syndromes. Additionally, identifying secondary forms further supports the hypothesis that WSS may stem from an autoimmune reaction targeting outer retinal antigens in susceptible individuals.

This review paper has provided a comprehensive overview of the different subtypes of WSS, presenting the latest advancements and interpretations in this field. Synthesizing the existing knowledge has shed light on the clinical manifestations, imaging findings, and proposed mechanisms underlying these disorders. The novel proposed staging systems outlined in the literature hold promise in facilitating accurate diagnosis, monitoring disease progression, and guiding treatment decisions for patients with WSS. However, further research and prospective studies are necessary to validate and refine these staging systems, as well as to explore potential therapeutic interventions for these complex and challenging conditions.

Author statement

Maria Vittoria Cicinelli: Conceptualization, Investigation, Writing – original draft, Writing – Reviewing & Editing. Percentage Contribution: 30%

Alessandro Marchese: Conceptualization, Investigation, Writing – original draft, Writing – Reviewing & Editing. Percentage Contribution: 20%

Prithvi Ramtohul: Conceptualization, Investigation, Writing – original draft, Writing – Reviewing & Editing. Percentage Contribution: 20%

K. Bailey Freund: Conceptualization, Writing – original draft, Writing – Reviewing & Editing, Supervision. Percentage Contribution: 5%

Francesco Bandello: Conceptualization, Writing – original draft, Writing – Reviewing & Editing, Supervision. Percentage Contribution: 5%

Elisabetta Miserocchi: Conceptualization, Investigation, Writing – original draft, Writing – Reviewing & Editing, Supervision. Percentage Contribution: 5%

Lee M. Jampol: Conceptualization, Investigation, Writing – original draft, Writing – Reviewing & Editing, Supervision. Percentage Contribution: 15%

Declaration of Generative AI and AI-assisted technologies in the writing process

During the preparation of this work the authors used chatGPT3.5 in order to improve readability and language of the manuscript. After using this tool/service, the authors reviewed and edited the content as needed and take full responsibility for the content of the publication.

Declaration of competing interest

The Authors have no competing interest in publishing the present

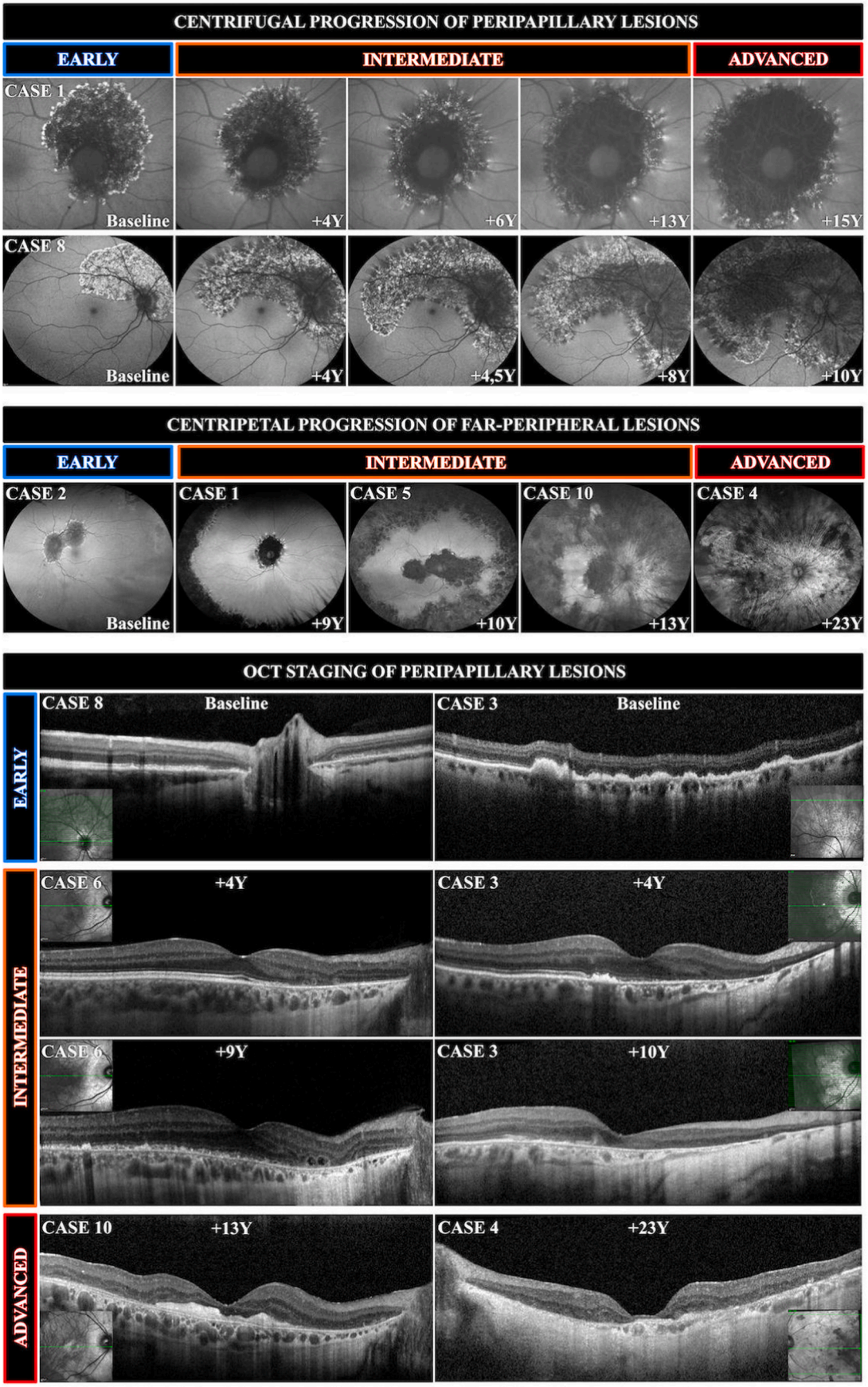

(caption on next page)

Fig. 17. Proposed disease staging of multizonal outer retinopathy and retinal pigment epitheliopathy (MORR) based on multimodal imaging correlation.
This figure presents a proposed staging system for multizonal outer retinopathy and retinal pigment epitheliopathy (MORR) based on ophthalmoscopic examination, fundus autofluorescence (FAF), and optical coherence tomography (OCT) imaging. The progression of lesions is classified into three distinctive stages: early, intermediate, and advanced. In the early stage, the peripapillary lesion exhibits a well-demarcated yellow-grey core of pigmentary alterations, corresponding to speckled hyperautofluorescence and disruption of the retinal pigment epithelium (RPE) and overlying ellipsoid/interdigitation zones (EZ/IZ) on FAF and OCT imaging, respectively. A thin demarcation line is observed, showing continuous hyperautofluorescence and focal RPE thickening with overlying EZ/IZ alteration on FAF and OCT imaging, respectively (first box). Far-peripheral regions display well-demarcated, 360-degree, annular zones of RPE atrophy, characterized by hypoautofluorescent areas bordered by a hyperautofluorescence line on FAF imaging. Mid-peripheral or macular skip lesions of RPE atrophy correspond to hypoautofluorescent lesions bordered by a hyperautofluorescence line (second box). In the intermediate stage, the peripapillary lesion demonstrates centrifugal progression, featuring a core of RPE depigmentation with increased visibility of the choroidal vasculature, corresponding to hypoautofluorescence and complete RPE atrophy on FAF and OCT imaging, respectively. The demarcation line is larger and interrupted, displaying fringe-like hyperautofluorescent features radiating outward, corresponding to focal RPE thickening on FAF and OCT imaging, respectively. Far-peripheral annular zones of RPE atrophy show centripetal progression, eventually merging with mid-peripheral or macular skip lesions. Far-peripheral lesions appear hypoautofluorescent and bordered by an interrupted demarcation line with fringe-like hyperautofluorescent features radiating inward. In the advanced stage, the peripapillary lesion exhibits a further centrifugal progression of RPE atrophy at the core, accompanied by hyperpigmentation. The hypoautofluorescent core expands, and the demarcation line thins with loss of the fringe-like hyperautofluorescent features, corresponding to complete RPE and outer retinal atrophy on FAF and OCT imaging, respectively. Far-peripheral lesions show further centripetal progression in a concentric pattern, display thinning of the hyperautofluorescent border with loss of the hyperautofluorescent features, and eventually merge with the peripapillary lesion, resulting in complete RPE and outer retinal degeneration. The loss of fringe-like hyperautofluorescent features within the demarcation lines indicates minimal lesion progression. The time point and case number are displayed for reference.

work.

Data availability

Data will be made available on request.

Acknowledgments

• a. Funding/Support: This research did not receive any specific grant from funding agencies in the public, commercial, or not-for-profit sectors. Prithvi Ramtohul is supported by The Philippe Foundation.

• b. Financial disclosures: Maria Vittoria Cicinelli, Alessandro Marchese, Prithvi Ramtohul, Elisabetta Miserocchi: No financial disclosures.

• Francesco Bandello consultant for: Allergan Inc (Irvine, California, USA), Bayer Shering-Pharma (Berlin, Germany), Hoffmann-La-Roche (Basel, Switzerland), Novartis (Basel, Switzerland), Sanofi-Aventis (Paris, France), Thrombogenics (Heverlee, Belgium), Zeiss (Dublin, USA), Boehringer-Ingelheim, Fidia Sooft, Ntc Pharma, Sifi

• K. Bailey Freund is a consultant for Heidelberg Engineering, Zeiss, Allergan, Bayer, Genentech, and Novartis and receives research support from Genentech/Roche.

• c. Other acknowledgments: None.

References

Aaberg, T.M., Campo, R.V., Joffe, L., 1985. Recurrences and bilaterality in the multiple evanescent white-dot syndrome. Am. J. Ophthalmol. 100, 29–37.
Abdelhakim, A.H., Yannuzzi, L.A., Freund, K.B., Jung, J.J., 2021. Differential response to glucocorticoid immunosuppression of two distinct inflammatory signs associated with punctate inner choroidopathy. Retina 41, 812–821.
Airaldi, M., Zicarelli, F., Forlani, V., Casaluci, M., Oldani, M., Staurenghi, G., Invernizzi, A., 2023. Correlation between inflammatory foci reactivation and atrophy growth in eyes with idiopathic multifocal choroiditis. Retina 43, 472–480.
Altan-Yaycioglu, R., Akova, Y.A., Akca, S., Yilmaz, G., 2006. Inflammation of the posterior uvea: findings on fundus fluorescein and indocyanine green angiography. Ocul. Immunol. Inflamm. 14, 171–179.
Amoroso, F., Mrejen, S., Pedinielli, A., Tabary, S., Souied, E.H., Gaudric, A., Cohen, S.Y., 2021. Intraretinal hyperreflective lines. Retina 41, 82–92.
Atan, D., Fraser-Bell, S., Plskova, J., Kuffova, L., Hogan, A., Tufail, A., Kilmartin, D.J., Forrester, J.V., Bidwell, J., Dick, A.D., Churchill, A.J., 2010. Cytokine polymorphism in noninfectious uveitis. Invest. Ophthalmol. Vis. Sci. 51, 4133–4142.
Atan, D., Fraser-Bell, S., Plskova, J., Kuffova, L., Hogan, A., Tufail, A., Kilmartin, D.J., Forrester, J.V., Bidwell, J.L., Dick, A.D., Churchill, A.J., 2011. Punctate inner choroidopathy and multifocal choroiditis with panuveitis share haplotypic associations with IL10 and TNF loci. Invest. Ophthalmol. Vis. Sci. 52, 3573–3581.
Bacci, T., Oh, D.J., Singer, M., Sadda, S., Freund, K.B., 2022. Ultra-widefield indocyanine green angiography reveals patterns of choroidal venous insufficiency influencing pachychoroid disease. Invest. Ophthalmol. Vis. Sci. 63, 17.
Baglivo, E., Safran, A.B., Borruat, F.X., 1996. Multiple evanescent white dot syndrome after hepatitis B vaccine. Am. J. Ophthalmol. 122, 431–432.
Barile, G.R., Harmon, S.A., 2017. Multiple evanescent white dot syndrome with central visual loss. Retin. Cases Brief Rep. 11 (Suppl. 1), S219–S225.
Battaglia Parodi, M., Iacono, P., Falcomata, B., Bolognesi, G., Bandello, F., 2015. Near-infrared fundus autofluorescence in multiple evanescent white-dot syndrome. Eur. J. Ophthalmol. 25, 43–46.
Battaglia Parodi, M., Iacono, P., Zucchiatti, I., Bandello, F., 2018. Choroidal neovascularization associated with multiple evanescent white dot syndrome treated with intravitreal ranibizumab. Ocul. Immunol. Inflamm. 26, 608–611.
Baumal, C.R., de Carlo, T.E., Waheed, N.K., Salz, D.A., Witkin, A.J., Duker, J.S., 2015. Sequential optical coherence tomographic angiography for diagnosis and treatment of choroidal neovascularization in multifocal choroiditis. JAMA Ophthalmol. 133, 1087–1090.
Bosello, F., Westcott, M., Casalino, G., Agorogiannis, G., Micciolo, R., Rees, A., Pavesio, C., 2022. Multiple evanescent white dot syndrome: clinical course and factors influencing visual acuity recovery. Br. J. Ophthalmol. 106, 121–127.
Boudreault, K.A., Schuerch, K., Zhao, J., Lee, W., Cabral, T., Yannuzzi, L.A., Tsang, S.H., Sparrow, J.R., 2017. Quantitative autofluorescence intensities in acute zonal occult outer retinopathy vs healthy eyes. JAMA Ophthalmol. 135, 1330–1338.
Bryan, R.G., Freund, K.B., Yannuzzi, L.A., Spaide, R.F., Huang, S.J., Costa, D.L., 2002. Multiple evanescent white dot syndrome in patients with multifocal choroiditis. Retina 22, 317–322.
Bujakowska, K., Audo, I., Mohand-Said, S., Lancelot, M.E., Antonio, A., Germain, A., Leveillard, T., Letexier, M., Saraiva, J.P., Lonjou, C., Carpentier, W., Sahel, J.A., Bhattacharya, S.S., Zeitz, C., 2012. CRB1 mutations in inherited retinal dystrophies. Hum. Mutat. 33, 306–315.
Cabral, D., Ramtohul, P., Zatreanu, L., Galhoz, D., Leitao, M., Nogueira, V., Sarraf, D., Freund, K.B., 2022. Deep capillary plexus features in acute macular neuroretinopathy: novel insights based on the anatomy of Henle fiber layer. Invest. Ophthalmol. Vis. Sci. 63, 4.
Cahuzac, A., Wolff, B., Mathis, T., Errera, M.H., Sahel, J.A., Mauget-Faysse, M., 2017. Multimodal imaging findings in 'hyper-early' stage MEWDS. Br. J. Ophthalmol. 101, 1381–1385.
Callanan, D., Gass, J.D., 1992. Multifocal choroiditis and choroidal neovascularization associated with the multiple evanescent white dot and acute idiopathic blind spot enlargement syndrome. Ophthalmology 99, 1678–1685.
Cantrill, H.L., Folk, J.C., 1986. Multifocal choroiditis associated with progressive subretinal fibrosis. Am. J. Ophthalmol. 101, 170–180.
Casalino, G., Introini, U., Pavesio, C.E., Bandello, F., 2017. Multimodal imaging features of resolving multiple evanescent white dot syndrome. Indian J. Ophthalmol. 65, 1209–1210.
Chang, A.A., Zhu, M., Billson, F., 2005. The interaction of indocyanine green with human retinal pigment epithelium. Invest. Ophthalmol. Vis. Sci. 46, 1463–1467.
Chao, D.L., Marsiglia, M., Ahmad, B., Sridhar, J., Shah, G.K., de Souza, E.C., Yannuzzi, L. A., Albini, T.A., 2015. Peripapillary serous detachment in multiple evanescent white dot syndrome. Retina 35, 521–524.
Chen, C., Cheng, Y., Zhang, Z., Zhang, Y., Xiao, Y., Peng, X., 2022. Clinical characteristics of streaky multifocal choroiditis: a subtype of multifocal choroiditis. Retina 42, 2110–2119.
Chen, K.C., Marsiglia, M., Dolz-Marco, R., Zahid, S., Mrejen, S., Pulido, J.S., Cohen, S.Y., Freilich, B., Yannuzzi, L.A., Freund, K.B., 2017. Foveal exudate and choroidal neovascularization in atypical cases of multiple evanescent white dot syndrome. Retina 37, 2025–2034.
Chen, Y., Chen, Q., Li, X., Li, M., 2021. RPE disruption and hyper-transmission are early signs of secondary CNV with punctate inner choroidopathy in structure-OCT. BMC Ophthalmol. 21, 427.
Cheung, C.M.G., Lee, W.K., Koizumi, H., Dansingani, K., Lai, T.Y.Y., Freund, K.B., 2019. Pachychoroid disease. Eye (Lond) 33, 14–33.
Cicinelli, M.V., Hassan, O.M., Gill, M.K., Goldstein, D., Parodi, M.B., Jampol, L.M., 2020a. A Multiple Evanescent White Dot Syndrome-like Reaction to Concurrent Retinal Insults. Ophthalmol Retina.
Cicinelli, M.V., Marchese, A., Bordato, A., Manitto, M.P., Bandello, F., Battaglia Parodi, M., 2020b. Reviewing the role of ultra-widefield imaging in inherited retinal dystrophies. Ophthalmol. Ther. 9, 249–263.

Cicinelli, M.V., Marchese, A., Ramtohul, P., Miserocchi, E., Introini, U., Bandello, F., Freund, K.B., Battaglia Parodi, M., 2022a. Punctate inner choroidopathy-like reactions in unrelated retinal diseases. Retina 42, 2099–2109.
Cicinelli, M.V., Miller, V., Marchese, A., Zaguia, F., Miserocchi, E., Goldstein, D.A., 2022b. Outer retinal disruption in early-onset birdshot chorioretinopathy. Ophthalmol. Retina 6, 863–865.
de Groot, E.L., Ten Dam-van Loon, N.H., Kouwenberg, C.V., de Boer, J.H., Ossewaarde-van Norel, J., 2023. Exploring imaging characteristics associated with disease activity in idiopathic multifocal choroiditis: a multimodal imaging approach. Am. J. Ophthalmol. 252, 45–58.
Dell'Omo, R., Mantovani, A., Wong, R., Konstantopoulou, K., Kulwant, S., Pavesio, C.E., 2010a. Natural evolution of fundus autofluorescence findings in multiple evanescent white dot syndrome: a long-term follow-up. Retina 30, 1479–1487.
Dell'omo, R., Wong, R., Marino, M., Konstantopoulou, K., Pavesio, C., 2010b. Relationship between different fluorescein and indocyanine green angiography features in multiple evanescent white dot syndrome. Br. J. Ophthalmol. 94, 59–63.
Dolz-Marco, R., Kalevar, A., McDonald, H.R., Cunningham Jr., E.T., Freund, K.B., 2021. Foveal outer retinal hyperreflectivity: a novel optical coherence tomography finding in idiopathic multifocal choroiditis. Retin. Cases Brief Rep. 15, 651–656.
Dreyer, R.F., Gass, D.J., 1984. Multifocal choroiditis and panuveitis. A syndrome that mimics ocular histoplasmosis. Arch. Ophthalmol. 102, 1776–1784.
Duncker, T., Lee, W., Jiang, F., Ramachandran, R., Hood, D.C., Tsang, S.H., Sparrow, J. R., Greenstein, V.C., 2018. Acute zonal occult outer retinopathy: structural and functional analysis across the transition zone between healthy and diseased retina. Retina 38, 118–127.
Dunlop, A.A., Cree, I.A., Hague, S., Luthert, P.J., Lightman, S., 1998. Multifocal choroiditis: clinicopathologic correlation. Arch. Ophthalmol. 116, 801–803.
Dutheil, C., Korobelnik, J.F., Delyfer, M.N., Rougier, M.B., 2018. Optical coherence tomography angiography and choroidal neovascularization in multifocal choroiditis: a descriptive study. Eur. J. Ophthalmol. 28, 614–621.
Dutta Majumder, P., Marchese, A., Pichi, F., Garg, I., Agarwal, A., 2020. An update on autoimmune retinopathy. Indian J. Ophthalmol. 68, 1829–1837.
Essex, R.W., Wong, J., Jampol, L.M., Dowler, J., Bird, A.C., 2013. Idiopathic multifocal choroiditis: a comment on present and past nomenclature. Retina 33, 1–4.
Essilfie, J., Bacci, T., Abdelhakim, A.H., Ramtohul, P., Turchi, F., Freund, K.B., Yannuzzi, L.A., 2022. Are there two forms of multiple evanescent white dot syndrome? Retina 42, 227–235.
Fekrat, S., Wilkinson, C.P., Chang, B., Yannuzzi, L., Schatz, H., Haller, J.A., 2000. Acute annular outer retinopathy: report of four cases. Am. J. Ophthalmol. 130, 636–644.
Ferrara, D.C., Merriam, J.E., Freund, K.B., Spaide, R.F., Takahashi, B.S., Zhitomirsky, I., Fine, H.F., Yannuzzi, L.A., Allikmets, R., 2008. Analysis of major alleles associated with age-related macular degeneration in patients with multifocal choroiditis: strong association with complement factor H. Arch. Ophthalmol. 126, 1562–1566.
Fine, H.F., Spaide, R.F., Ryan Jr., E.H., Matsumoto, Y., Yannuzzi, L.A., 2009. Acute zonal occult outer retinopathy in patients with multiple evanescent white dot syndrome. Arch. Ophthalmol. 127, 66–70.
Finn, A.P., Khurana, R.N., 2021. Multiple evanescent white dot syndrome: bilateral disease may be silent and asymmetric. Am. J. Ophthalmol. Case Rep. 21, 101004.
Flage, T., Sand, A.B., Syrdalen, P., 1977. Haemorrhagic maculopathy in young adults. Acta Ophthalmol. 55, 489–496.
Francis, P.J., Marinescu, A., Fitzke, F.W., Bird, A.C., Holder, G.E., 2005. Acute zonal occult outer retinopathy: towards a set of diagnostic criteria. Br. J. Ophthalmol. 89, 70–73.
Freund, K.B., Mrejen, S., Jung, J., Yannuzzi, L.A., Boon, C.J., 2013. Increased fundus autofluorescence related to outer retinal disruption. JAMA Ophthalmol. 131, 1645–1649.
Fujiwara, T., Imamura, Y., Giovinazzo, V.J., Spaide, R.F., 2010. Fundus autofluorescence and optical coherence tomographic findings in acute zonal occult outer retinopathy. Retina 30, 1206–1216.
Fung, A.T., Sorenson, J.A., Freund, K.B., 2012. An atypical white dot syndrome after traumatic subretinal hemorrhage. Retin. Cases Brief Rep. 6, 339–344.
Gal-Or, O., Priel, E., Rosenblatt, I., Shulman, S., Kramer, M., 2017. Multimodal imaging in an unusual cluster of multiple evanescent white dot syndrome. J. Ophthalmol. 2017, 7535320.
Gal-Or, O., Sorenson, J.A., Gattoussi, S., Dolz-Marco, R., Freund, K.B., 2019. Multiple evanescent white dot syndrome with subretinal deposits. Retin. Cases Brief Rep. 13, 314–319.
Gan, Y., Zhang, X., Chen, L., Wen, F., 2020. Intraretinal cystoid spaces in regression of punctate inner choroidopathy lesions. Ocul. Immunol. Inflamm. 28, 938–946.
Gargouri, M.A., Yousfi, N., Toutain, J., Fares, S., Lejoyeux, R., Gabison, E., Cochereau, I., Titah, C., Azar, G., 2022. Multiple evanescent white dot syndrome following COVID-19 mRNA vaccination. Ocul. Immunol. Inflamm. 1–5.
Gass, J.D., 1993. Acute zonal occult outer retinopathy. Donders lecture: The Netherlands ophthalmological society, Maastricht, Holland, June 19, 1992. J. Clin. Neuro Ophthalmol. 13, 79–97.
Gass, J.D., Agarwal, A., Scott, I.U., 2002. Acute zonal occult outer retinopathy: a long-term follow-up study. Am. J. Ophthalmol. 134, 329–339.
Gass, J.D., Hamed, L.M., 1989. Acute macular neuroretinopathy and multiple evanescent white dot syndrome occurring in the same patients. Arch. Ophthalmol. 107, 189–193.
Gass, J.D., Stern, C., 1995. Acute annular outer retinopathy as a variant of acute zonal occult outer retinopathy. Am. J. Ophthalmol. 119, 330–334.
Gattoussi, S., Ghadiali, Q., Dolz-Marco, R., Freund, K.B., 2018. Idiopathic multifocal choroiditis presenting with a transient peripapillary white ring. Retin. Cases Brief Rep. 12 (Suppl. 1), S81–S86.
Gaudric, A., Mrejen, S., 2017. Why the dots are black only in the late phase of the indocyanine green angiography in multiple evanescent white dot syndrome. Retin. Cases Brief Rep. 11 (Suppl. 1), S81–S85.
Gerstenblith, A.T., Thorne, J.E., Sobrin, L., Do, D.V., Shah, S.M., Foster, C.S., Jabs, D.A., Nguyen, Q.D., 2007. Punctate inner choroidopathy: a survey analysis of 77 persons. Ophthalmology 114, 1201–1204.
Gilbert, R.M., Niederer, R.L., Kramer, M., Sharief, L., Sharon, Y., Bar, A., Lightman, S., Tomkins-Netzer, O., 2020. Differentiating multifocal choroiditis and punctate inner choroidopathy: a cluster analysis approach. Am. J. Ophthalmol. 213, 244–251.
Giuffre, C., Marchese, A., Fogliato, G., Miserocchi, E., Modorati, G.M., Sacconi, R., Cicinelli, M.V., Miere, A., Amoroso, F., Capuano, V., Souied, E., Bandello, F., Querques, G., 2021. The "Sponge sign": a novel feature of inflammatory choroidal neovascularization. Eur. J. Ophthalmol. 31, 1240–1247.
Gliem, M., Birtel, J., Muller, P.L., Hendig, D., Faust, I., Herrmann, P., Holz, F.G., Adamus, G., Charbel Issa, P., 2019a. Acute retinopathy in pseudoxanthoma elasticum. JAMA Ophthalmol. 137, 1165–1173.
Gliem, M., Birtel, J., Muller, P.L., Hendig, D., Faust, I., Herrmann, P., Holz, F.G., Adamus, G., Charbel Issa, P., 2019b. Acute retinopathy in pseudoxanthoma elasticum. JAMA Ophthalmol. 137, 1165–1173, 2019.
Golshani, C., Gal-Or, O., Giovinazzo, V., Freund, K.B., 2020. An elderly patient with acute transient outer retinal disruption resembling bilateral multiple evanescent white dot syndrome. Retin. Cases Brief Rep. 14, 131–136.
Grewal, D.S., Fishman, G.A., Jampol, L.M., 2014. Autoimmune retinopathy and antiretinal antibodies: a review. Retina 34, 827–845.
Gross, N.E., Yannuzzi, L.A., Freund, K.B., Spaide, R.F., Amato, G.P., Sigal, R., 2006. Multiple evanescent white dot syndrome. Arch. Ophthalmol. 124, 493–500.
Haas, A.M., Stattin, M., Ahmed, D., Krebs, I., Ansari-Shahrezaei, S., 2020. Development of secondary choroidal neovascularization in focal choroidal excavation of punctate inner choroidopathy. Ocul. Immunol. Inflamm. 28, 20–25.
Hady, S.K., Xie, S., Freund, K.B., Cunningham Jr., E.T., Wong, C.W., Cheung, C.M.G., Kamoi, K., Igarashi-Yokoi, T., Ali, O.M., Wasfi, E.I., Rateb, M.F., Ohno-Matsui, K., 2022. Prevalence and characteristics of multifocal choroiditis/punctate inner choroidopathy in pathologic myopia eyes with patchy atrophy. Retina 42, 669–678.
Haen, S.P., Spaide, R.F., 2008. Fundus autofluorescence in multifocal choroiditis and panuveitis. Am. J. Ophthalmol. 145, 847–853.
Hamed, L.A., Schatz, N.J., Glaser, J.S., Gass, J.D., 1988. Acute idiopathic blind spot enlargement without optic disc edema. Arch. Ophthalmol. 106, 1030–1031.
Hamed, L.M., Glaser, J.S., Gass, J.D., Schatz, N.J., 1989. Protracted enlargement of the blind spot in multiple evanescent white dot syndrome. Arch. Ophthalmol. 107, 194–198.
Hashimoto, H., Kishi, S., 2015. Ultra-wide-field fundus autofluorescence in multiple evanescent white dot syndrome. Am. J. Ophthalmol. 159, 698–706.
Hoang, Q.V., Cunningham Jr., E.T., Sorenson, J.A., Freund, K.B., 2013a. The "pitchfork sign" a distinctive optical coherence tomography finding in inflammatory choroidal neovascularization. Retina 33, 1049–1055.
Hoang, Q.V., Gallego-Pinazo, R., Yannuzzi, L.A., 2013b. Long-term follow-up of acute zonal occult outer retinopathy. Retina 33, 1325–1327.
Introini, U., Casalino, G., Dhrami-Gavazi, E., Mukkamala, S.K., Mrejen, S., Schubert, H., Cohen, S.Y., Azzolini, C., Bandello, F., Chang, S., Yannuzzi, L.A., 2018. Clinical course of acute zonal occult outer retinopathy complicated by choroidal neovascularization. Int. J. Retina Vitreous 4, 32.
Jain, A., Shilpa, I.N., Biswas, J., 2022. Multiple evanescent white dot syndrome following SARS-CoV-2 infection - a case report. Indian J. Ophthalmol. 70, 1418–1420.
Jampol, L.M., Sieving, P.A., Pugh, D., Fishman, G.A., Gilbert, H., 1984. Multiple evanescent white dot syndrome. I. Clinical findings. Arch. Ophthalmol. 102, 671–674.
Jampol, L.M., Tauscher, R., Schwarz, H.P., 2021. COVID-19, COVID-19 vaccinations, and subsequent abnormalities in the retina: causation or coincidence? JAMA Ophthalmol. 139, 1135–1136.
Jung, J.J., Khan, S., Mrejen, S., Gallego-Pinazo, R., Cunningham Jr., E.T., Freund, K.B., Jampol, L.M., Yannuzzi, L.A., 2014. Idiopathic multifocal choroiditis with outer retinal or chorioretinal atrophy. Retina 34, 1439–1450.
Kaden, T.R., Gattoussi, S., Dolz-Marco, R., Balaratnasingam, C., Yannuzzi, L.A., Freund, K.B., 2019. The nature and frequency of outer retinal disruption in idiopathic multifocal choroiditis associated with persistent fundus hyperautofluorescence. Ophthalmic Surg. Lasers Imag. Retina 50, 675–683.
Kang, H.G., Kim, T.Y., Kim, M., Byeon, S.H., Kim, S.S., Koh, H.J., Lee, S.C., Lee, C.S., 2022. Expanding the clinical spectrum of multiple evanescent white dot syndrome with overlapping multifocal choroiditis. Ocul. Immunol. Inflamm. 30, 81–89.
Kim, H., Woo, S.J., Kim, Y.K., Lee, S.C., Lee, C.S., 2015. Focal choroidal excavation in multifocal choroiditis and punctate inner choroidopathy. Ophthalmology 122, 1534–1535.
Kongwattananon, W., Grasic, D., Lin, H., Oyeniran, E., Sen, H.N., Kodati, S., 2022. Role of optical coherence tomography angiography in detecting and monitoring inflammatory choroidal neovascularization. Retina 42, 1047–1056.
Kramer, M., Priel, E., 2014. Fundus autofluorescence imaging in multifocal choroiditis: beyond the spots. Ocul. Immunol. Inflamm. 22, 349–355.
Krill, A.E., Chishti, M.I., Klien, B.A., Newell, F.W., Potts, A.M., 1969. Multifocal inner choroiditis. Trans. Am. Acad. Ophthalmol. Otolaryngol. 73, 222–245.
Labriola, L.T., Legarreta, A.D., Legarreta, J.E., Nadler, Z., Gallagher, D., Hammer, D.X., Ferguson, R.D., Iftimia, N., Wollstein, G., Schuman, J.S., 2016. Imaging with multimodal adaptive-optics optical coherence tomography in multiple evanescent white dot syndrome: the structure and functional relationship. Retin. Cases Brief Rep. 10, 302–309.

Lafaut, B.A., Loeys, B., Leroy, B.P., Spileers, W., De Laey, J.J., Kestelyn, P., 2001. Clinical and electrophysiological findings in autosomal dominant vitreoretinochoroidopathy: report of a new pedigree. Graefes Arch. Clin. Exp. Ophthalmol. 239, 575–582.
Levine, J.P., Freund, K.B., Cooney, M.J., Klancnik Jr., J.M., Shirkey, B.L., Yannuzzi, L.A., 2008. Multifocal choroiditis in siblings. Retin. Cases Brief Rep. 2, 151–153.
Li, D., Kishi, S., 2007. Loss of photoreceptor outer segment in acute zonal occult outer retinopathy. Arch. Ophthalmol. 125, 1194–1200.
Li, D., Kishi, S., 2009. Restored photoreceptor outer segment damage in multiple evanescent white dot syndrome. Ophthalmology 116, 762–770.
Li, M., Zhang, X., Wen, F., 2015. The fundus autofluorescence spectrum of punctate inner choroidopathy. J. Ophthalmol. 2015, 202097.
Lin, B.R., Russell, J.F., Al-Khersan, H., Goldhardt, R., 2022. A systematic review of acute zonal occult outer retinopathy with a focus on attempted treatment modalities. Curr. Ophthalmol. Rep. 10, 168–178.
Liu, N., Wu, N., Cicinelli, M.V., Fawzi, A.A., 2021. Diagnostic and therapeutic challenges. Retina 41, 1780–1785.
Mabchour, A., Motulsky, E., Kisma, N., 2023. Active ocular toxoplasmosis associated with simultaneous multiple evanescent white dot syndrome. Ocul. Immunol. Inflamm. 1–4.
Mahajan, V.B., Stone, E.M., 2010. Patients with an acute zonal occult outer retinopathy-like illness rapidly improve with valacyclovir treatment. Am. J. Ophthalmol. 150, 511–518.
Makino, S., Tanaka, Y., Tampo, H., 2013. An optical coherence tomography and fundus autofluorescence imaging study of peripapillary acute zonal occult outer retinopathy. Case Rep. Ophthalmol. 4, 11–16.
Mantovani, A., Invernizzi, A., Staurenghi, G., Herbort Jr., C.P., 2019. Multiple evanescent white dot syndrome: a multimodal imaging study of foveal granularity. Ocul. Immunol. Inflamm. 27, 141–147.
Marchese, A., Agarwal, A.K., Erba, S., Scialdone, A., Miserocchi, E., Bandello, F., Introini, U., Jampol, L.M., Casalino, G., 2022a. Placoid lesions of the retina: progress in multimodal imaging and clinical perspective. Br. J. Ophthalmol. 106, 14–25.
Marchese, A., Arrigo, A., Bandello, F., Parodi, M.B., 2018a. Peripheral linear streaks in pseudoxanthoma elasticum. Ophthalmic Surg. Lasers Imag. Retina 49, e292–e295.
Marchese, A., Cicinelli, M.V., Cavalleri, M., Bandello, F., Modorati, G., Miserocchi, E., 2022b. Chorioretinal atrophy in vitreoretinal lymphoma: risk factors and visual outcomes. Retina 42, 561–568.
Marchese, A., Romano, F., Cicinelli, M.V., Bandello, F., Battaglia Parodi, M., 2018b. Chorioretinal punched-out lesions in pseudoxanthoma elasticum. Retina 38, e43–e44.
Marchese, A., Agarwal, A., Moretti, A.G., Handa, S., Modorati, G., Querques, G., Bandello, F., Gupta, V., Miserocchi, E., 2020. Advances in imaging of uveitis. Ther. Adv. Ophthalmol. 12.
Marsiglia, M., Gallego-Pinazo, R., Cunha de Souza, E., Munk, M.R., Yu, S., Mrejen, S., Cunningham Jr., E.T., Lujan, B.J., Goldberg, N.R., Albini, T.A., Gaudric, A., Francais, C., Rosen, R.B., Freund, K.B., Jampol, L.M., Yannuzzi, L.A., 2016. Expanded clinical spectrum of multiple evanescent white dot syndrome with multimodal imaging. Retina 36, 64–74.
Mathis, T., Delaunay, B., Cahuzac, A., Vasseur, V., Mauget-Faysse, M., Kodjikian, L., 2018. Choroidal neovascularisation triggered multiple evanescent white dot syndrome (MEWDS) in predisposed eyes. Br. J. Ophthalmol. 102, 971–976.
Mathis, T., Delaunay, B., Favard, C., Denis, P., Kodjikian, L., 2020. HYPERAUTOFLUORESCENT SPOTS IN ACUTE OCULAR TOXOPLASMOSIS: A New Indicator of Outer Retinal Inflammation. Retina.
Meng, Y., Zhang, Q., Li, L., Yi, Z., Xu, Y., Su, Y., Liang, C., Xiao, D., Zhang, L., Chen, C., 2023. Primary Multiple Evanescent White Dot Syndrome (MEWDS) and MEWDS Secondary to Multifocal Choroiditis/punctate Inner Choroidopathy: A Comparative Study. Retina.
Meredith, T.A., Smith, R.E., Braley, R.E., Witkowski, J.A., Koethe, S.M., 1978. The prevalence of HLA-B7 in presumed ocular histoplasmosis in patients with peripheral atrophic scars. Am. J. Ophthalmol. 86, 325–328.
Merino, D., Duncan, J.L., Tiruveedhula, P., Roorda, A., 2011. Observation of cone and rod photoreceptors in normal subjects and patients using a new generation adaptive optics scanning laser ophthalmoscope. Biomed. Opt Express 2, 2189–2201.
Miyata, M., Ooto, S., Muraoka, Y., 2022. Punctate inner choroidopathy immediately after COVID-19 infection: a case report. BMC Ophthalmol. 22, 297.
Mkrtchyan, M., Lujan, B.J., Merino, D., Thirkill, C.E., Roorda, A., Duncan, J.L., 2012. Outer retinal structure in patients with acute zonal occult outer retinopathy. Am. J. Ophthalmol. 153, 757–768, 768 e751.
Monson, D.M., Smith, J.R., 2011. Acute zonal occult outer retinopathy. Surv. Ophthalmol. 56, 23–35.
Morgan, C.M., Schatz, H., 1986. Recurrent multifocal choroiditis. Ophthalmology 93, 1138–1147.
Moussa, K., Alsberge, J.B., Munk, M.R., Vora, R.A., Emami-Naeini, P., Yiu, G., Cunningham Jr., E.T., 2022. Idiopathic multifocal choroiditis with serpiginous-like peripapillary chorioretinal atrophy. Retina 42, 1574–1582.
Mrejen, S., Khan, S., Gallego-Pinazo, R., Jampol, L.M., Yannuzzi, L.A., 2014. Acute zonal occult outer retinopathy: a classification based on multimodal imaging. JAMA Ophthalmol. 132, 1089–1098.
Munk, M.R., Jung, J.J., Biggee, K., Tucker, W.R., Sen, H.N., Schmidt-Erfurth, U., Fawzi, A.A., Jampol, L.M., 2015. Idiopathic multifocal choroiditis/punctate inner choroidopathy with acute photoreceptor loss or dysfunction out of proportion to clinically visible lesions. Retina 35, 334–343.
Nakao, S., Kaizu, Y., Oshima, Y., Sakamoto, T., Ishibashi, T., Sonoda, K.H., 2016. Optical coherence tomography angiography for detecting choroidal neovascularization secondary to punctate inner choroidopathy. Ophthalmic Surg. Lasers Imag. Retina 47, 1157–1161.
Nakao, S., Kaizu, Y., Yoshida, S., Iida, T., Ishibashi, T., 2015. Spontaneous remission of acute zonal occult outer retinopathy: follow-up using adaptive optics scanning laser ophthalmoscopy. Graefes Arch. Clin. Exp. Ophthalmol. 253, 839–843.
Ng, C.C., Jumper, J.M., Cunningham Jr., E.T., 2020. Multiple evanescent white dot syndrome following influenza immunization - a multimodal imaging study. Am. J. Ophthalmol. Case Rep. 19, 100845.
Nozik, R.A., Dorsch, W., 1973. A new chorioretinopathy associated with anterior uveitis. Am. J. Ophthalmol. 76, 758–762.
Oh, K.T., Folk, J.C., Maturi, R.K., Moore, P., Kardon, R.H., 2001. Multifocal electroretinography in multifocal choroiditis and the multiple evanescent white dot syndrome. Retina 21, 581–589.
Olsen, T.W., Capone Jr., A., Sternberg Jr., P., Grossniklaus, H.E., Martin, D.F., Aaberg, T. M., 1996. Subfoveal choroidal neovascularization in punctate inner choroidopathy. Surgical management and pathologic findings. Ophthalmology 103, 2061–2069.
Ong, A.Y., Birtel, J., Agorogiannis, E., Sharma, S.M., Charbel Issa, P., 2023. Topographic patterns of retinal lesions in multiple evanescent white dot syndrome. Graefes Arch. Clin. Exp. Ophthalmol.
Ongkosuwito, J.V., Kortbeek, L.M., Van der Lelij, A., Molicka, E., Kijlstra, A., de Smet, M. D., Suttorp-Schulten, M.S., 1999. Aetiological study of the presumed ocular histoplasmosis syndrome in The Netherlands. Br. J. Ophthalmol. 83, 535–539.
Onishi, A.C., Roberts, P.K., Jampol, L.M., Nesper, P.L., Fawzi, A.A., 2019. Characterization and correlation of "Jampol dots" on adaptive optics with foveal granularity on conventional fundus imaging. Retina 39, 235–246.
Pachydaki, S.I., Jakobiec, F.A., Bhat, P., Sobrin, L., Michaud, N.A., Seshan, S.V., D'Amico, D.J., 2012. Surgical management and ultrastructural study of choroidal neovascularization in punctate inner choroidopathy after bevacizumab. J. Ophthalmic Inflamm. Infect. 2, 29–37.
Palestine, A.G., Nussenblatt, R.B., Parver, L.M., Knox, D.L., 1984. Progressive subretinal fibrosis and uveitis. Br. J. Ophthalmol. 68, 667–673.
Pang, C.E., Shah, V.P., Sarraf, D., Freund, K.B., 2014. Ultra-widefield imaging with autofluorescence and indocyanine green angiography in central serous chorioretinopathy. Am. J. Ophthalmol. 158, 362–371 e362.
Papadia, M., Herbort, C.P., 2010. Idiopathic choroidal neovascularisation as the inaugural sign of multiple evanescent white dot syndrome. Middle East Afr. J. Ophthalmol. 17, 270–274.
Park, D.W., Polk, T.D., Stone, E.M., 1997. Multiple evanescent white dot syndrome in a patient with Best disease. Arch. Ophthalmol. 115, 1342–1343.
Parnell, J.R., Jampol, L.M., Yannuzzi, L.A., Gass, J.D., Tittl, M.K., 2001. Differentiation between presumed ocular histoplasmosis syndrome and multifocal choroiditis with panuveitis based on morphology of photographed fundus lesions and fluorescein angiography. Arch. Ophthalmol. 119, 208–212.
Pearlman, R.B., Golchet, P.R., Feldmann, M.G., Yannuzzi, L.A., Cooney, M.J., Thorne, J. E., Folk, J.C., Ryan, E.H., Agarwal, A., Barnes, K.C., Becker, K.G., Jampol, L.M., 2009. Increased prevalence of autoimmunity in patients with white spot syndromes and their family members. Arch. Ophthalmol. 127, 869–874.
Pece, A., Allegrini, D., Kontadakis, S., Querques, G., Rossetti, L., 2016. Intravitreal ranibizumab for choroidal neovascularization in a patient with angioid streaks and multiple evanescent white dots. BMC Ophthalmol. 16, 122.
Pichi, F., Srvivastava, S.K., Chexal, S., Lembo, A., Lima, L.H., Neri, P., Saitta, A., Chhablani, J., Albini, T.A., Nucci, P., Freund, K.B., Chung, H., Lowder, C.Y., Sarraf, D., 2016. EN face optical coherence tomography and optical coherence tomography angiography of multiple evanescent white dot syndrome: new insights into pathogenesis. Retina 36 (Suppl. 1), S178–S188.
Ramakrishnan, M.S., Patel, A.P., Melles, R., Vora, R.A., 2021. Multiple evanescent white dot syndrome: findings from a large Northern California cohort. Ophthalmol. Retina 5, 850–854.
Ramtohul, P., Cabral, D., Cicinelli, M.V., Freund, K.B., 2022a. Recurrence of acute retinopathy in pseudoxanthoma elasticum. Retin. Cases Brief Rep.
Ramtohul, P., Cabral, D., Oh, D., Galhoz, D., Freund, K.B., 2023a. En face ultrawidefield OCT of the vortex vein system in central serous chorioretinopathy. Ophthalmol. Retina 7, 346–353.
Ramtohul, P., Cabral, D., Sadda, S., Freund, K.B., Sarraf, D., 2022b. The OCT angular sign of Henle fiber layer (HFL) hyperreflectivity (ASHH) and the pathoanatomy of the HFL in macular disease. Prog. Retin. Eye Res., 101135
Ramtohul, P., Cicinelli, M.V., Dolz-Marco, R., Gal-Or, O., Mrejen, S., Garcia-Martinez, J. R., Goldberg, A., Cunha de Souza, E., Miserocchi, E., Cunningham Jr., E.T., Yannuzzi, L.A., Freund, K.B., Tsui, E., 2023b. The Chrysanthemum Phenotype of Idiopathic Multifocal Choroiditis. Retina.
Ramtohul, P., Gascon, P., Denis, D., 2020. Outer retinal plume signature in multiple evanescent white dot syndrome. Ophthalmol. Retina 4, 766.
Riaz, K.M., Jampol, L.M., Mirza, R.G., 2012. Fundus autofluorescence imaging in punctate inner choroidopathy with blind spot enlargement. Ocul. Immunol. Inflamm. 20, 460–463.
Saraux, H., Pelosse, B., Guigui, A., 1986. [Multifocal inner choroiditis: pseudohistoplasmosis. The European form of the presumed American histoplasmosis]. J. Fr. Ophtalmol. 9, 645–651.
Scharf, J.M., Hilely, A., Freund, K.B., Sarraf, D., 2022. Autofluorescent timeline of spots and dots in multiple evanescent white dot syndrome. Retin. Cases Brief Rep. 16, 280–284.
Seetharam, S.S., Jampol, L.M., Gill, M.K., 2015. New insights into acute annular outer retinopathy. Retin. Cases Brief Rep. 9, 1–6.
Seong, H.J., Lee, C.S., 2022. Multiple evanescent white dot syndrome with submacular fluid in dome-shaped macula following COVID-19 vaccination: a case report. Kor. J. Ophthalmol. 36, 471–473.

Serrar, Y., Cahuzac, A., Gascon, P., Langlois-Jacques, C., Mauget-Faysse, M., Wolff, B., Seve, P., Kodjikian, L., Mathis, T., 2022. Comparison of primary and secondary forms of multiple evanescent white dot syndrome. Retina 42, 2368–2378.
Shelsta, H.N., Rao, R.R., Bhatt, H.K., Jampol, L.M., 2011. Atypical presentations of multiple evanescent white dot syndrome without white dots: a case series. Retina 31, 973–976.
Shi, X., Cai, Y., Luo, X., Liang, S., Rosenfeld, P.J., Li, X., 2020. Presence or absence of choroidal hyper-transmission by SD-OCT imaging distinguishes inflammatory from neovascular lesions in myopic eyes. Graefes Arch. Clin. Exp. Ophthalmol. 258, 751–758.
Shimada, H., Yuzawa, M., Hirose, T., Nakashizuka, H., Hattori, T., Kazato, Y., 2008. Pathological findings of multifocal choroiditis with panuveitis and punctate inner choroidopathy. Jpn. J. Ophthalmol. 52, 282–288.
Sieving, P.A., Fishman, G.A., Jampol, L.M., Pugh, D., 1984. Multiple evanescent white dot syndrome. II. Electrophysiology of the photoreceptors during retinal pigment epithelial disease. Arch. Ophthalmol. 102, 675–679.
Slakter, J.S., Giovannini, A., Yannuzzi, L.A., Scassellati-Sforzolini, B., Guyer, D.R., Sorenson, J.A., Spaide, R.F., Orlock, D., 1997. Indocyanine green angiography of multifocal choroiditis. Ophthalmology 104, 1813–1819.
Smith, P.D., 1999. Neutrophil activation and mediators of inflammation in chronic venous insufficiency. J. Vasc. Res. 36 (Suppl. 1), 24–36.
Smith, R.E., Ganley, J.P., 1972. Presumed ocular histoplasmosis. I. Histoplasmin skin test sensitivity in cases identified during a community survey. Arch. Ophthalmol. 87, 245–250.
Soifer, M., Nguyen, N.V., Leite, R., Fernandes, J., Kodati, S., 2022. Recurrent multiple evanescent white dot syndrome (MEWDS) following first dose and booster of the mRNA-1273 COVID-19 vaccine: case report and review of literature. Vaccines (Basel) 10.
Spaide, R.F., 2004. Collateral damage in acute zonal occult outer retinopathy. Am. J. Ophthalmol. 138, 887–889.
Spaide, R.F., Goldberg, N., Freund, K.B., 2013. Redefining multifocal choroiditis and panuveitis and punctate inner choroidopathy through multimodal imaging. Retina 33, 1315–1324.
Spaide, R.F., Lally, D.R., 2021. High resolution spectral domain optical coherence tomography of multiple evanescent white dot syndrome. Retin. Cases Brief Rep.
Spaide, R.F., Skerry, J.E., Yannuzzi, L.A., DeRosa, J.T., 1990. Lack of the HLA-DR2 specificity in multifocal choroiditis and panuveitis. Br. J. Ophthalmol. 74, 536–537.
Standardization of Uveitis Nomenclature Working, G., 2021a. Classification criteria for multifocal choroiditis with panuveitis. Am. J. Ophthalmol. 228, 152–158.
Standardization of Uveitis Nomenclature Working, G., 2021b. Classification criteria for punctate inner choroiditis. Am. J. Ophthalmol. 228, 275–280.
Sugawara, E., Machida, S., Fujiwara, T., Kurosaka, D., Hayakawa, M., 2010. Punctate inner choroidopathy in mother and daughter. Jpn. J. Ophthalmol. 54, 505–507.
Thompson, I.A., Caplash, S., Akanda, M., Sabbagh, O., Choan, B., Cheng, S.K., Okeagu, C., Sen, H.N., 2021. Optical coherence tomography angiography changes in choroidal vasculature following treatment in punctate inner choroidopathy. Ocul. Immunol. Inflamm. 29, 944–950.
Thorne, J.E., Wittenberg, S., Jabs, D.A., Peters, G.B., Reed, T.L., Kedhar, S.R., Dunn, J.P., 2006. Multifocal choroiditis with panuveitis incidence of ocular complications and of loss of visual acuity. Ophthalmology 113, 2310–2316.
Tsai, L., Jampol, L.M., Pollock, S.C., Olk, J., 1994. Chronic recurrent multiple evanescent white dot syndrome. Retina 14, 160–163.
Turkcuoglu, P., Chang, P.Y., Rentiya, Z.S., Channa, R., Ibrahim, M., Hatef, E., Sophie, R., Sadaka, A., Wang, J., Sepah, Y.J., Do, D.V., Foster, C.S., Nguyen, Q.D., 2011. Mycophenolate mofetil and fundus autofluorescence in the management of recurrent punctate inner choroidopathy. Ocul. Immunol. Inflamm. 19, 286–292.
Vadala, M., Lodato, G., Cillino, S., 2001. Multifocal choroiditis: indocyanine green angiographic features. Ophthalmologica 215, 16–21.
Vadboncoeur, J., Jampol, L.M., Goldstein, D.A., 2022. Acute zonal occult outer retinopathy: a case report of regression after an intravitreal dexamethasone (ozurdex) implant. Retin. Cases Brief Rep. 16, 466–469.
Vance, S.K., Freund, K.B., Wenick, A.S., Nguyen, Q.D., Holland, G.N., Kreiger, A.E., 2011a. Diagnostic and therapeutic challenges. Retina 31, 1224–1230.
Vance, S.K., Khan, S., Klancnik, J.M., Freund, K.B., 2011b. Characteristic spectral-domain optical coherence tomography findings of multifocal choroiditis. Retina 31, 717–723.
Veronese, C., Maiolo, C., Morara, M., Armstrong, G.W., Ciardella, A.P., 2018. Bilateral multiple evanescent white dot syndrome. Int. Ophthalmol. 38, 2153–2158.
Wang, L., Lankry, P., Rabinovitch, D., Gallo, R., Laiginhas, R., Iyer, P., Shulman, S., Trivizki, O., 2022. An elderly man with atypical multiple evanescent white dot syndrome. Case Rep. Ophthalmol. 13, 892–896.
Wang, Q., Jiang, L., Yan, W., Wei, W., Lai, T.Y.Y., 2017. Fundus autofluorescence imaging in the assessment of acute zonal occult outer retinopathy. Ophthalmologica 237, 153–158.
Watzke, R.C., Packer, A.J., Folk, J.C., Benson, W.E., Burgess, D., Ober, R.R., 1984. Punctate inner choroidopathy. Am. J. Ophthalmol. 98, 572–584.
Wiley, Z.C., Pakravan, M., Charoenkijkajorn, C., Kavoussi, S.C., Lee, A.G., 2022. Uveomeningeal syndrome presenting with bilateral optic disc edema and multiple evanescent white dots syndrome (MEWDS). Am. J. Ophthalmol. Case Rep. 26, 101538.
Williams, L.B., Javed, A., Sabri, A., Morgan, D.J., Huff, C.D., Grigg, J.R., Heng, X.T., Khng, A.J., Hollink, I., Morrison, M.A., Owen, L.A., Anderson, K., Kinard, K., Greenlees, R., Novacic, D., Nida Sen, H., Zein, W.M., Rodgers, G.M., Vitale, A.T., Haider, N.B., Hillmer, A.M., Ng, P.C., Shankaracharya, Cheng, A., Zheng, L., Gillies, M.C., van Slegtenhorst, M., van Hagen, P.M., Missotten, T., Farley, G.L., Polo, M., Malatack, J., Curtin, J., Martin, F., Arbuckle, S., Alexander, S.I., Chircop, M., Davila, S., Digre, K.B., Jamieson, R.V., DeAngelis, M.M., 2019. ALPK1 missense pathogenic variant in five families leads to ROSAH syndrome, an ocular multisystem autosomal dominant disorder. Genet. Med. 21, 2103–2115.
Woods, A.C., Wahlen, H.E., 1959. The probable role of Benign histoplasmosis in the etiology of granulomatous uveitis. Trans. Am. Ophthalmol. Soc. 57, 318–343.
Wyhinny, G.J., Jackson, J.L., Jampol, L.M., Caro, N.C., 1990. Subretinal neovascularization following multiple evanescent white-dot syndrome. Arch. Ophthalmol. 108, 1384–1385.
Xu, Q.A., Athwal, A., Heisler, M., Ju, M.J., Vanzan, V., Ferrara, D., Sarunic, M., Navajas, E.V., 2022. Adaptive optics optical coherence tomography in a case of acute zonal occult outer retinopathy. Retin. Cases Brief Rep. 16, 435–438.
Yang, C.S., Hsieh, M.H., Su, H.I., Kuo, Y.S., 2019. Multiple evanescent white dot syndrome following acute Epstein-Barr Virus infection. Ocul. Immunol. Inflamm. 27, 244–250.
Yenerel, N.M., Kucumen, B., Gorgun, E., Dinc, U.A., 2008. Atypical presentation of multiple evanescent white dot syndrome (MEWDS). Ocul. Immunol. Inflamm. 16, 113–115.
Zahid, S., Chen, K.C., Jung, J.J., Balaratnasingam, C., Ghadiali, Q., Sorenson, J., Rofagha, S., Freund, K.B., Yannuzzi, L.A., 2017. Optical coherence tomography angiography of chorioretinal lesions due to idiopathic multifocal choroiditis. Retina 37, 1451–1463.
Zarranz-Ventura, J., Sim, D.A., Keane, P.A., Patel, P.J., Westcott, M.C., Lee, R.W., Tufail, A., Pavesio, C.E., 2014. Characterization of punctate inner choroidopathy using enhanced depth imaging optical coherence tomography. Ophthalmology 121, 1790–1797.
Zhang, X., Zuo, C., Li, M., Chen, H., Huang, S., Wen, F., 2013. Spectral-domain optical coherence tomographic findings at each stage of punctate inner choroidopathy. Ophthalmology 120, 2678–2683.
Zicarelli, F., Mantovani, A., Preziosa, C., Staurenghi, G., 2020. Multimodal imaging of multiple evanescent white dot syndrome: a new interpretation. Ocul. Immunol. Inflamm. 28, 814–820.